2014

Test development to determine the feasibility of rubber tractor treads for use as blasting mats

Matthew Kurtis Coy

Department:

TEST DEVELOPMENT TO DETERMINE THE FEASIBILITY OF RUBBER TRACTOR TREADS FOR USE AS BLASTING MATS

by

MATTHEW KURTIS COY

A THESIS

Presented to the Faculty of the Graduate School of the

MISSOURI UNIVERSITY OF SCIENCE AND TECHNOLOGY

In Partial Fulfillment of the Requirements for the Degree

MASTER OF SCIENCE IN EXPLOSIVES ENGINEERING

2014

Approved by

Paul N. Worsey

Jason Baird

Richard L. Bullock

ABSTRACT

The objective of this thesis was to determine if rubber tractor treads could be used as an alternative material for blasting mats. These treads are made from steel cable and vulcanized rubber and are very tough. However, once they reach the end of their life on mobile equipment, they are destined for a landfill, or dump site because they are too tough to recycle. A potential alternative use for them is as blasting mats.

An examination of existing mat designs was conducted to better understand the matting methods used by the blasting industry today, to learn from those designs allow a higher quality blasting mat to be made.

Because there was no standardized test for assessing mat performance, a test was created. A flyrock study was performed to quantify the forces produced during blasting. A standard blast testing procedure was established for mats of different designs and allowed the tractor tread mat's performance to be compared with the common current industry standard. Once the mat was constructed, it was tested through rigorous blasting. The blast test was set up specifically to provide realistic blasting conditions that mats need to endure.

The mats performed very well and with a few improvements in fastener design, the tractor tread mat withstood the blasting forces better than the control mat. This thesis also establishes a standard for judging the performance of new mat materials in the future.

ACKNOWLEDGMENTS

Thanks to Dr. Worsey and the faculty at MS&T for the opportunities to expand my education and improve myself, Dr. Baird for lending me the Phantom camera for my testing and to the MS&T Experimental Mine staff, Jimmie Taylor and DeWayne Phelps, for aiding me in performing my testing and helping me learn better techniques to use my testing time more effectively. Thanks to those who donated equipment to this research: **Dave Kolb Grading** for donating the treads, **Brunner & Lay** for drill steel and bits, **Buckley Powder Co**. for dynamite and blasting caps, and **Twehouse Construction** for letting me spectacularly destroy your blasting mat, and giving me the cable to construct the tractor tread mat. Thanks to my undergraduate assistants Joe Cook, Jenna Freese, and David Frimpong. You guys helped me do my testing in some really hot, or in Joe's case, really cold conditions.

TABLE OF CONTENTS

LIST OF ILLUSTRATIONS

Page

LIST OF TABLES

Page

1. INTRODUCTION

1.1 GENERAL INFORMATION

In the commercial blasting industry, flying rocks and debris as a result of blasting can become a hazard when in close proximity to property such as houses, highways, or other areas where people are present or property damage is a likely result. The term flyrock is used to describe the rocks and debris that leave a blast site as the result of blasting operations. Blasting mats are used in the commercial blasting industry to prevent or reduce incidents where flyrock presents a hazard. Blasting mats are constructed of resilient materials and placed over a blast pattern to reduce and eliminate risks to lives and property that would result from flyrock produced during a blast.

1.2 VARIETY OF BLASTING MATS

Blasting mats come in many sizes and materials. Small mats can be comprised of chain link, woven cable, or other lightweight, flexible material. The advantage of these smaller mats is their ability to be easily transported due to their light weight and flexibility. However, they are limited by their lack of weight. Small blasting mats are not as effective in larger blasting applications due to the larger volumes of flyrock generated during the blast. In contrast to small mats, most of the larger mats are comprised of some combination of rubber tire and cable. Large mats usually require heavy equipment such as front end loaders and track hoes to move them into place for a blast and remove them once the blast has been shot.

1.3 POTENTIAL ALTERNATIVE BLASTING MAT MATERIALS

With many different ways to construct a blast mat come the possibilities of the use of other materials in mat construction. Dave Kolb Grading, a construction company based out of St. Charles, MO, asked if the MST Experimental Mine superintendent could make use of damaged rubber tractor treads. These retired tractor treads were taken off of large mobile equipment, mostly large agricultural tractors, because they were damaged beyond repair and rendered unusable. According to Sydenstricker John Deere salesman Brent Thomas, who manages sales of tracked John Deere equipment in Northeast

Missouri, there are about 4 large tractor treads of similar size to the ones used in this project, sold or replaced per year. Sydenstricker also sells or replaces up to 30 of the smaller sized tracks used on skid loaders (Thomas, 2014). When these treads are replaced, they are typically discarded in a landfill, or stacked in a corner of an equipment yard and left. The goals of this thesis were to build a blast mat from rubber tractor treads and develop a test to determine its viability. A standardized test for blasting mats had not been previously developed for the evaluation of new designs and/or materials.

2. PREVIOUS WORK

2.1 BLAST MAT DESIGNS

As stated in the introduction, there are many different ways a blasting mat can be constructed. The most common form is some variant of rubber tires that are stacked on top of one another and steel cables or wire rope threaded perpendicularly through them to bind them together. Different versions of this array include using the treaded section of a discarded tire for the mat, the sidewalls of a discarded tire for the mat, and using plates in place of tires. Eleven patent filings were examined related to different blasting mat designs. Some of these designs are very similar while there are a few unique solutions. Evaluation of these methods provided a starting point for the construction of the rubber tractor tread blast mats. The different mats are discussed and critiqued by first examining existing mat designs, and then selecting key design elements unique to those mats to incorporate in the constructed tractor tread mat in Section 4.

2.1.1. Belanger Rubber Tire Mats. In 1967, L. Belanger received a patent for his blasting mat. This patent, U.S. Patent No. 3,331,322, claimed the use of used rubber tires, cut into 120 degree sections around the radius, and the tread section then removed from the sidewalls in strips. These strips and curved pieces were hole-punched, stacked, interwoven with separate steel cables running longitudinally through the mat, then plated and bolted into place on the ends. Figure 2.1, from Belanger's patent, shows the details of the mat materials, bindings, and the assembled mat (Belanger).

The Belanger design is the basis for many of the current blast mat designs in use. It provided a well-built, heavy blasting mat that could hold together through the rigors of blasting operations. It was described as a solution to more dangerous and ineffective practices used in the blasting industry at that time. Previous methods mentioned in the patent include laying pipes, girders, or timbers over a blast to absorb energy and control flyrock. These methods were inefficient in stopping flyrock and sometimes caused hazards of their own, not limited to flying pipes, girders, and timbers. A mat needed to be built not only to withstand the blast, but be constructed so its components do not become a hazard if the mat should fail. The Belanger design prevents this by bulking up the mats with sections of rubber tire. This was accomplished by stacking all the tire

sections on edge, rather than arranging them in a flat configuration. Arranging the tires in this way leaves small voids where the tires do not line up completely, allowing explosive gasses to be transmitted through. These apertures are still small enough that they do not allow harmful sized rock fragments through the mat. Another advantage of this arrangement is the amount of material that is placed in between the blast and the cables that bind the mat together. This extra material protects the cables from direct impact and wear from abrasion (Belanger).

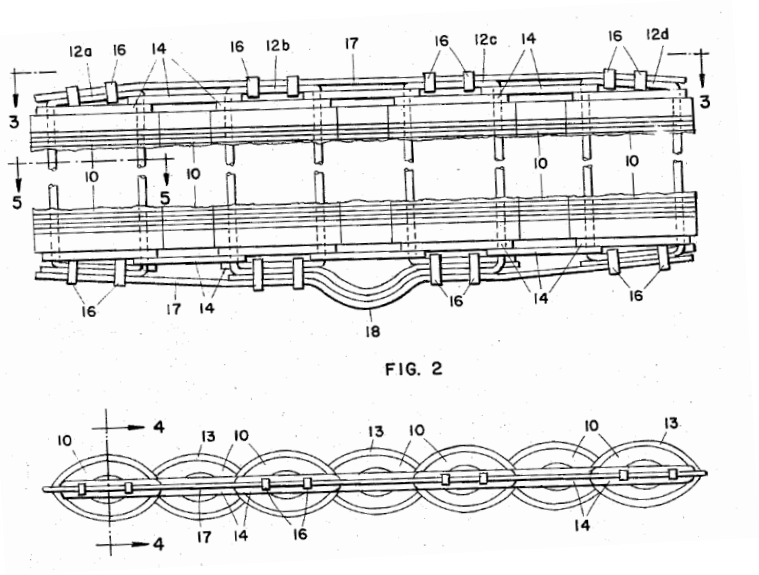

Figure 2.1 Belanger Mat Profile and Side View (Belanger)

Altogether, Belanger presented a solid design and it has stood the test of time. Many of the current blast mats follow this general form. However, as with any manmade creation, there are some disadvantages. The main disadvantage is due to the strongest part of the mat, the cables. While steel cable itself is a strong material, orientation of the surrounding material can work against it. With Belanger's design, the cables run the length of the mat and meet at the ends. This means whatever pulling or stretching force is encountered is divided amongst those main cables. A failure in one of these cables will

result in that load being divided amongst those remaining, and so on. The tensile load on the cables worsens with each failure. And although Belanger's design is resilient, resisting blast forces means that material failure is not a matter of if, but when. For a blast mat, failure of one of the cables that bind the mat could cause multiple problems. The first, more immediate problem is the possibility of rock fragments of significant size penetrating the mat and leaving the blast site. The second problem deals more with the utilization of the mat. If the cable is broken, the operator must consider whether it is worth the time and man-hours to repair the mat or to obtain a new one.

The use of tire strips raises problems for cable longevity as well. The tire strips are there to protect the cables from rock fragments and add bulk to the mat. To the mat's detriment, they also raise the cables off of the mat and provide a fulcrum for the ends of the mat to further stress the cables when resisting a blast load. The tire strips in between the cables and the blast will stay together at a focal point above the blast, but the cables above will be stressed more due to the ends of the mat stretching the cables around an arc. Figure 2.2 is an example of this stretching. The mat's binding cable is represented in green and the area with the most stretching stress is highlighted in red.

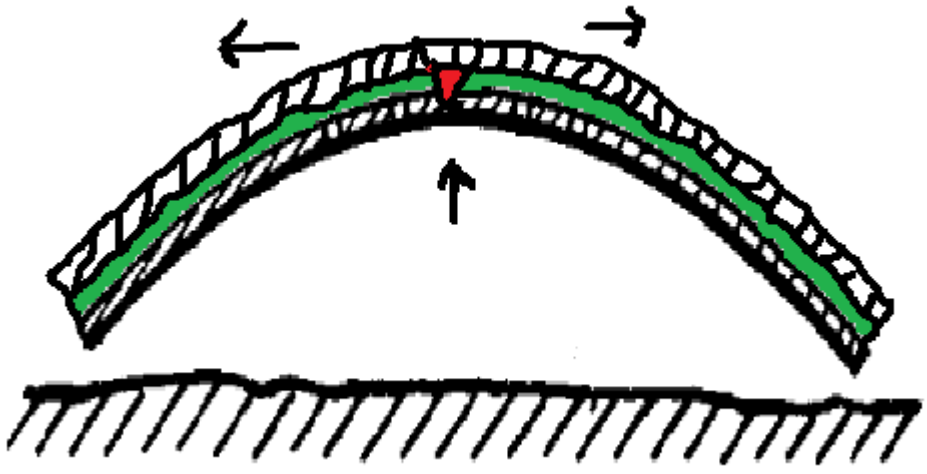

Figure 2.2 Stretching Forces on a Belanger Blasting Mat by Author

The stretching process is further agitated with the addition of dirt and mud from the blast site. Mats are often dragged through mud, dirt, and other media that can settle in the cracks between the mats. This adds weight to the mat and also adds stretching forces on the cables. The more foreign media that gets caught in these apertures, the more volume is taken up. These actions continually stretch the cables until they reach their failure point. Corrosion of these cables can also develop as a result of moisture and foreign materials built up in the mat. It is imperative to the life of the mats that they be kept clean of debris and stored in a dry place. As long as blasting mats designed in this manner are properly maintained, they will last for a long time.

2.1.2. Wikner Pipe and Cable Mats. The 1968 U.S. patent, No. 3371604, filed by Folke Wikner claimed the construction of a blasting mat composed of woven cable and pipes made of a "resilient material." Most materials used to construct blasting mats are recycled and repurposed materials that have been damaged or worn past their limit for their originally intended purpose. Most cables, tires, and other components become feasible for use as blasting mat materials because they are no longer new and can be acquired for significantly less money. The reason these materials were originally replaced is because they either lost their integrity or in the case of cables, reached a point that their failure could occur with further use. In this document Wikner suggested the manufacturing of this mat from new materials. Wikner describes a woven and interlaced cable array that traces its way through parallel pipes of some sort of durable material. Polymer pipes were suggested as a possibility. These pipes gave the mat form and shape, while the exposed sections of cable that bound the mat were able to stay flexible. The largest advantage of this mat is its lightweight construction and flexibility which allows it to be easily transported from one worksite to another without the need for heavy equipment. It can be rolled up and tied and then transported to the next job. Gasses can easily pass through this mat because the apertures between pipes are very long, giving them the ability to open up under high pressure. Mats built this way are also easily cleaned as there is less material and spaces for dirt to get trapped in. Figure 2.3 shows the blast mat design patented by Wikner (Wikner).

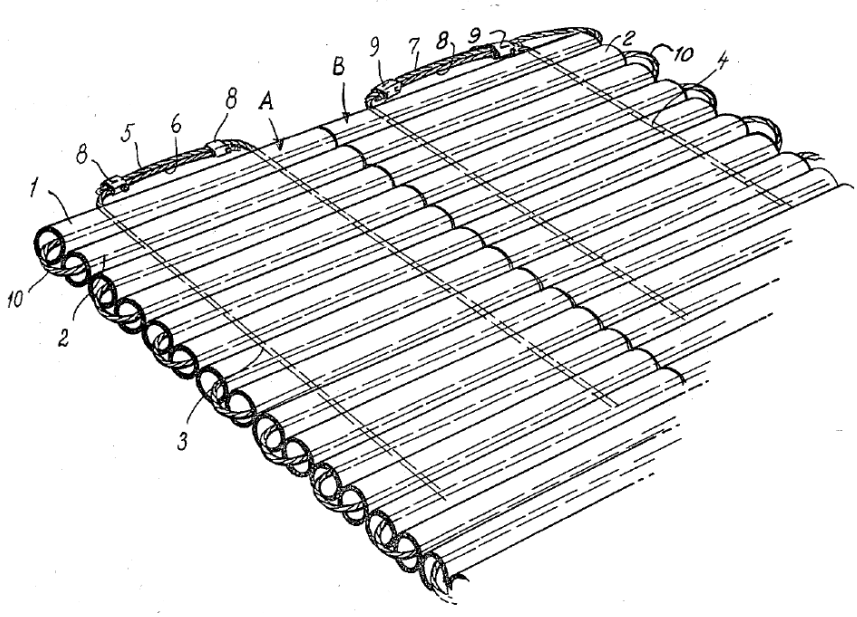

Figure 2.3 Wikner Pipe and Cable Isometric View (Wikner)

Disadvantages to this type of mat are mainly related to its light weight and composition. The lack of bulk provides little to oppose high-velocity material trying to leave a blast site. The flexibility of the mat keeps it together so it can envelop the flyrock, but it will not stay on top of the site as readily as other designs. Also, if the mat is not centered over the blast, it can be flipped off to the side where it would be useless. Cables are also an essential part of the design of this mat. If one were to break, large portions of the mat could become unstrung. This mat design is recommended for smaller scale blasts to be able to fully utilize the equipment.

2.1.3. Berg Wire-Ring Mats. Eric Berg received a patent, No. 3539135, for a wire-ring blast mat in 1970. This mat differed in design from previous mats in that it did not use any rigid parts. Berg's design for this blast mat consisted of large wire rings that were interlocked like chain-mail. This mat allows generated gasses to escape easily while trapping rock particles larger than the size of the wire rings. Like the pipe-and-cable mats, this design allows for the mats to be rolled up and easily transported, as well as

moved around without the need for heavy equipment. Figure 2.4 shows the form of this type of blasting mat (Berg).

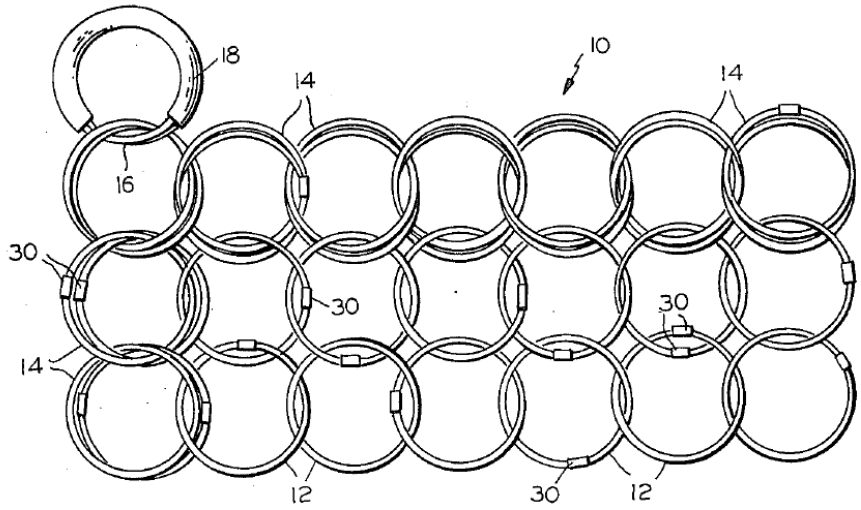

Figure 2.4 Berg Wire Ring Blasting Mat (Berg)

This design works similar to placing chain-link fence over a blast, with the exception that if one of the links is damaged, the whole mat does not pull apart. This design overcomes the downfall of the previous two designs in that there are not one or two key material sections tying the entire mat together. If a link is damaged, it can be repaired with minimal effort. This design is easy to clean because there are not gaps for material to get stuck in as easily. Material caught in the mat would likely be close to the size of the rings and easily removed. However, smaller material could pass through this type of mat unhindered.

Berg's design suffers from the same shortfall as the pipe-and-cable mat in that it has very little mass. If the mat is not of sufficient length and width, it will be useless. This mat must have dimensions extending beyond the blast radius to provide extra material to enclose larger flyrock particles once they become airborne. The extra material covers the sides so flyrock cannot escape around the mat. This is another design that works best on small blasts.

2.1.4. Bomb Blanket. This design of blasting mat was patented by Arthur Cunn in 1972, U.S. Patent No. 3648613. It is a square ballistic cloth with strips of flexible reinforcing material stretching diagonally to the corners of the mat. When the charge goes off, it propels the mat upward. Because of the reinforced sections stretching to the corners, the extra material creates fold points so that the mat folds around the projected material. This is shown below in Figure 2.5 (Cunn).

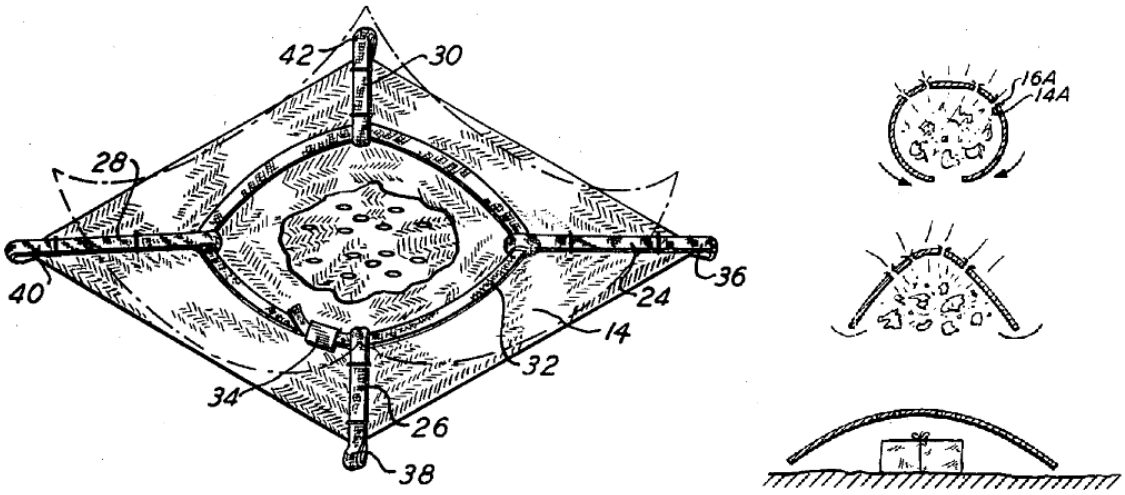

Figure 2.5 Cunn Bomb Blanket (Cunn)

This mat was designed mostly for military applications, such as working with landmines, but it could also have applications in small blasts. The main point to take away from this design is not the material it is made of, but the fact that it is designed to fold on purpose and capture the material. This mat design isn't big enough to be of much use in larger mining operations, but is claimed it could be effective in small cratering blasts (Cunn).

2.1.5. Cable and Plate Mats. Lewis' 1974 design of blasting mats is very similar to the design produced by Belanger earlier. It was given a separate U.S. patent, No. 3793953. Instead of tire pieces, plates of unspecified resilient material are used. These

plates comprise the bulk of blasting mats made with this design. The plates are block-like with squared ends (Lewis). This opens up the apertures between the plates so gasses can permeate more freely. This is shown in Figure 2.6 with a side by side comparison of the Belanger design on the left, and the Lewis design on the right.

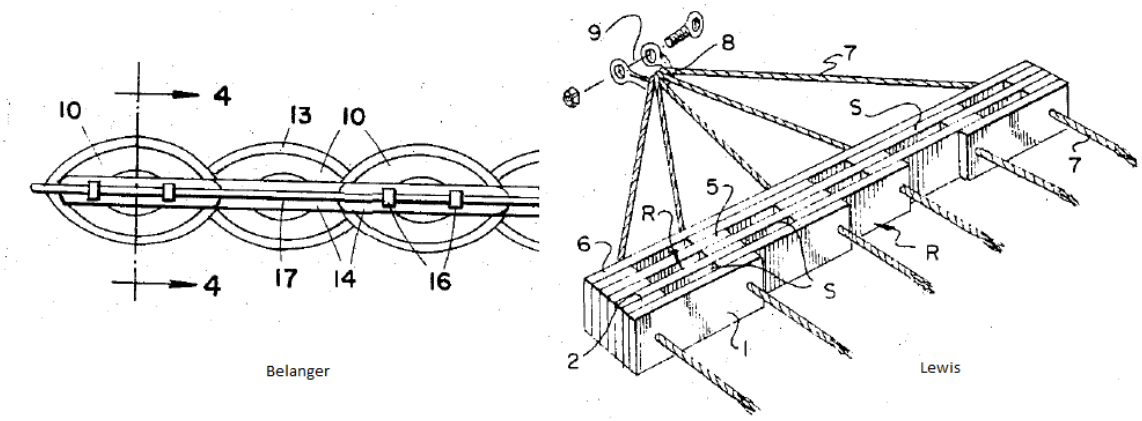

Figure 2.6 Belanger and Lewis Comparison (Belanger) (Lewis)

The plates should not be made so thick that the apertures are large enough to allow flyrock to penetrate. This type of mat can be useful on large blasts like the Belanger style mats, but still suffers the detriment of main cables binding it together. The mat can pick up a lot of dirt similar to the Belanger mats and be difficult to keep clean and free of debris.

2.1.6. Woven Cable Mats. In the 1975 Patent No. 3870256, woven cable mats designed by John A. and Joseph S. Mazella incorporate only steel cable and associated fasteners. This is the second steel cable blasting mat patent submitted by Joseph S. Mazella. This patent has the cables interlaced so the cable spacing is equal on all sides. In his previous design, U.S. Patent 2474904, the cables were woven together similar to a loomed material. The steel cables are interlaced with each other and the ends fastened to an outer ring of cable to serve as the edge of the mat as shown in Figure 2.7.

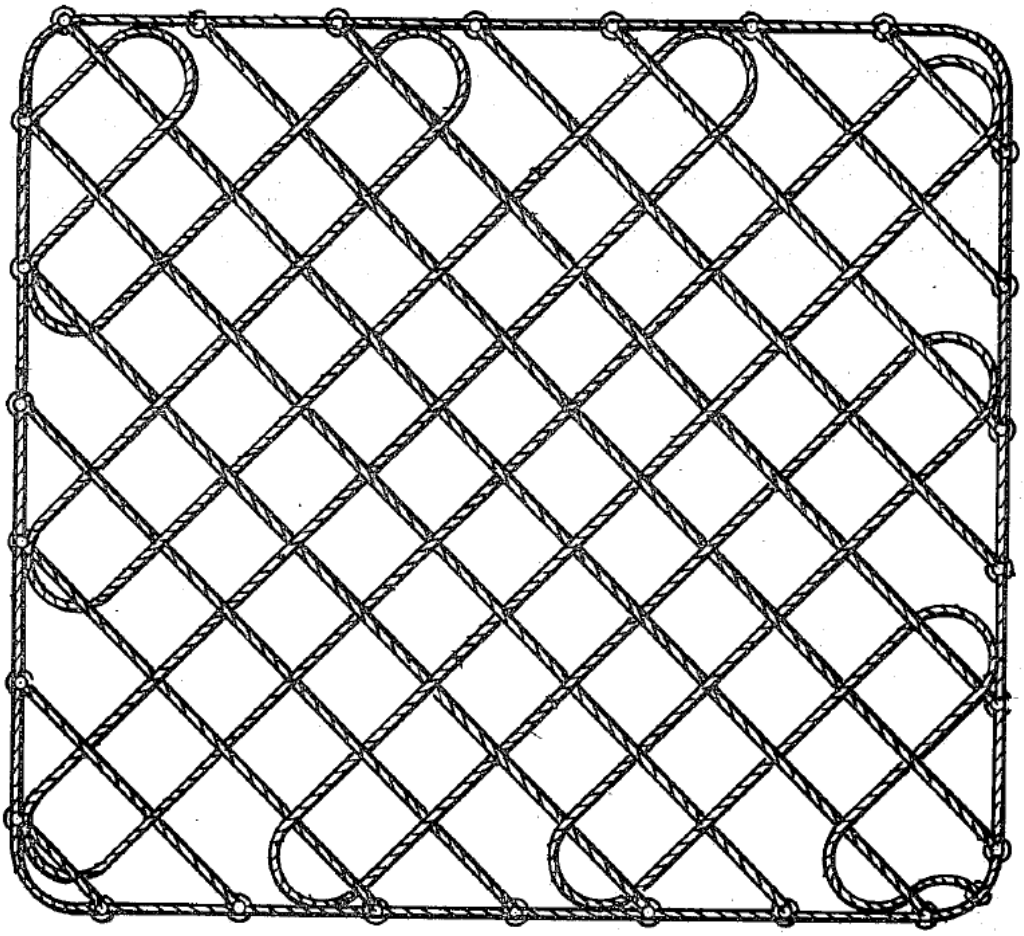

Figure 2.7 Woven Cable Mat, U.S. Patent 3870256 (Mazella)

This design resembles a fishnet pattern. The advantages of this mat are that it is lightweight and easily transported. The lack of material means that it is easy to clean and maintain as well. The main shortcomings to this are the weight and how the cables are interwoven. The Mazellas' design allows the cables to move around during blasting which can create larger holes than were originally in the mat. The shifting of the cables will not damage them but it can let rock particles through the mat (Mazella).

2.1.7. Modular Rubber Tire Mat. The 1976 rubber tire mat designed by Robertson, Patent No. 3943853, has approximately the same material orientation and binding as the Belanger design. The difference in this patent is that it proposes sections of mats to be built with a bolt together design. This would allow for mats to be sized

appropriately for the job at hand. Larger mats could be assembled by bolting shorter sections together, and vice versa. Figure 2.8 shows a cross section of this sort of mat with the linkage points for bolting sections together highlighted in green. This greatly aids in the portability of the mats and allows for smaller equipment to be able to move the mats into place on blasts where larger mats are required (Robertson). However, this design never obtained popularity. This is probably due to the difficulty in attaching mats together using this method.

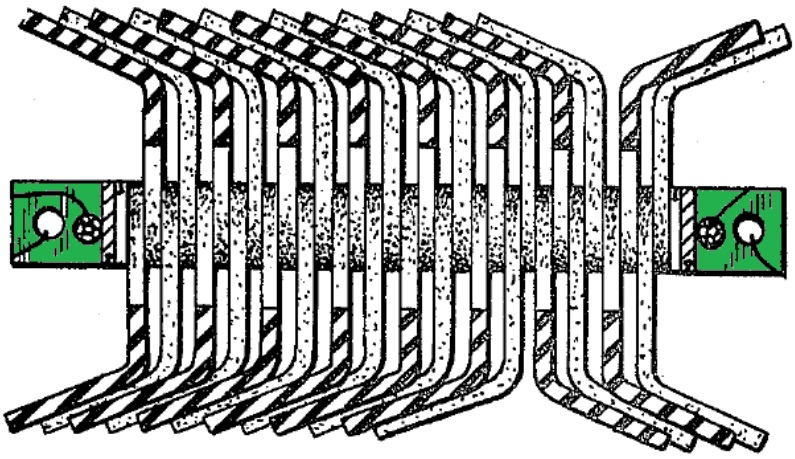

Figure 2.8 Modular Rubber Tire Mat Section (Robertson, 1976)

2.1.8. Modular Block Mat. Another U.S. patent, No. 3945319, was issued in 1976 for modular mat. This mat, designed by Meagher, is comprised of blocks of material that are bolted together. These blocks are long and rectangular. Rather than the modular rubber-tire mat designed by Robertson, Meagher's design is a rigid mat, shown in Figure 2.9.

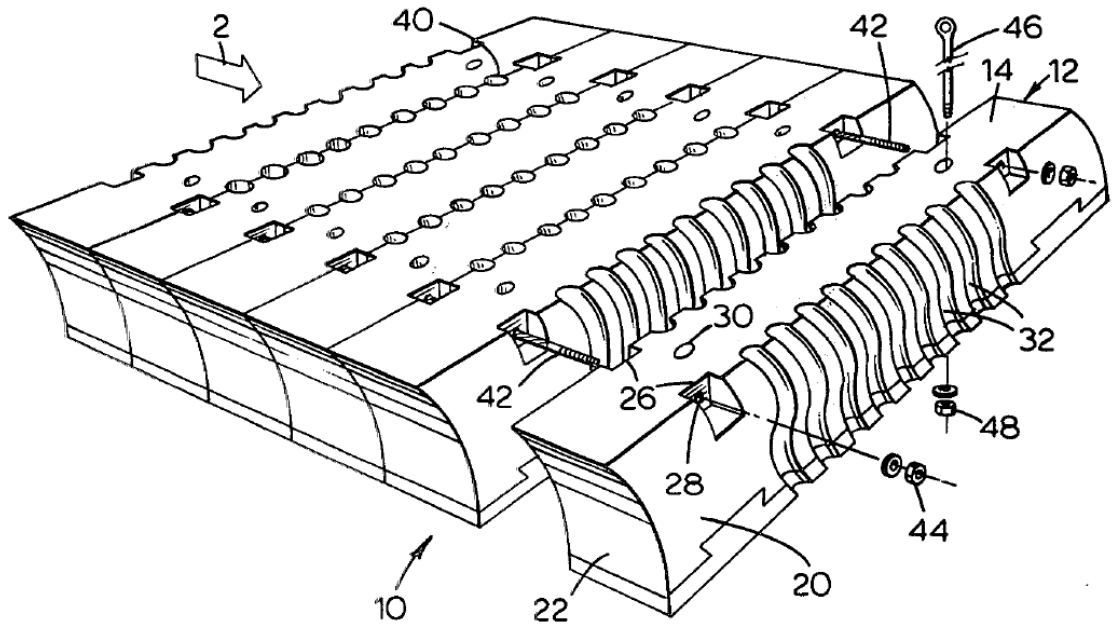

Figure 2.9 Meagher Modular Block Mat Design (Meagher)

The blocks bolt together tightly with no gaps in between except for vent holes molded into the sides that butt together. With this, there are no large apertures for material to go through, the mats have plenty of bulk, and they can be assembled to the required size for the job (Meagher). Cleanup is easy since most trapped materials will fall out upon disassembly. Two disadvantages for this are the need to purchase or manufacture the blocks in large numbers and deal with the long setup times and hardware. The main downfall with using this type of mat is the need to piece it together and take it apart, and the cost of that associated man-power. It is cumbersome and time consuming.

2.1.9. Rubber Tire Sidewall Mat. The mat design submitted by Leo Arcand who was granted a patent in 1982, U.S. Patent No. 4315463, is very similar to the Belanger design. Rather than quartering the sidewalls of the tires, this mat design uses the entire sidewall in a complete ring (Arcand). The design of this mat is thicker than the Belanger form, providing more weight per square foot than its predecessor. It also has more places where dirt and rocks can become lodged between the tires. A side view of this mat design is shown in Figure 2.10.

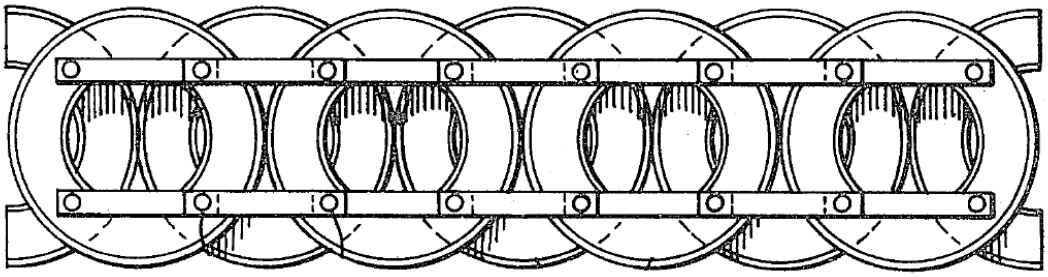

Figure 2.10 Rubber Tire Sidewall Mat (Arcand)

2.1.10. Rubber Tire Sidewall Ring Mat. Patent No. 4801217, granted to Jerry Goldberg in 1989, described a blasting mat that was comprised of the sidewalls and beads of the tire, but rather than the Belanger layout, the rings are arrayed similar to the design produced by Berg. The rings are arrayed so that they cover a large area using minimal resources. However, unlike Berg's design, the rings are not interwoven, but bound every 90 degrees by strips of material. Goldberg suggests using tire strips with their ends tied in a square knot should be used to bind the rings together (Goldberg). Figure 2.11 shows a comparison of Goldberg's mat design alongside Berg's design.

The two may look similar but the material and binding methods are different. Goldberg's design does not have as much strength in its fasteners and cannot have interlocking rings. Scale is not stated in either patent, but the wire rings that comprise Berg's mat design can be made much smaller than the rings made from tire sidewalls, which would be around 16-18" inner diameter. The primary purpose of this mat is not a blasting mat, but a means to secure a path over unstable ground for farming or logging equipment. While the author states the device may be used in blasting operations, it is not the invention's main purpose (Goldberg). For blasting operations, the holes in the center of the beads, where wheels would go, would allow large amounts of debris through. The solution to this would be to layer multiple mats and offset them so that the gaps are bisected by the next mat.

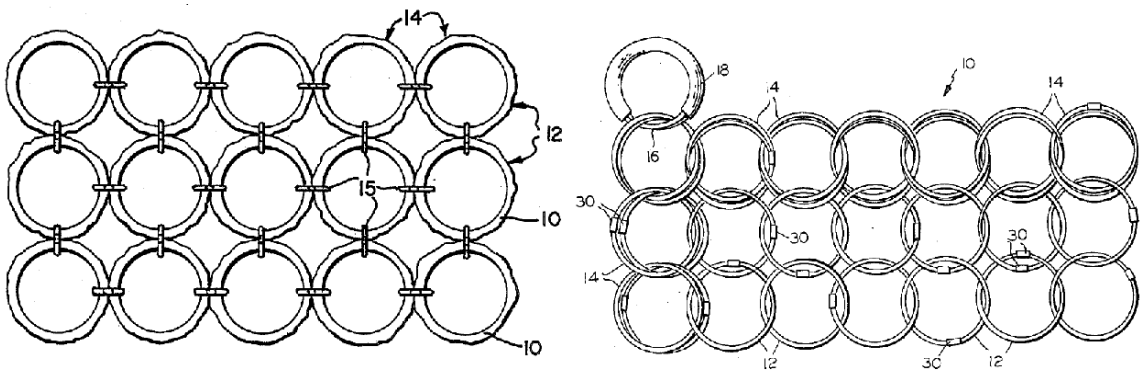

Figure 2.11 Goldberg and Berg Comparison

2.1.11. Tire Tread Mat. Patent No. 5482754, granted in 1966 to Carol Cook, is yet another rubber tire mat in similar form to the Belanger design. The only difference here is the use of just the tread portion of the tire instead of the sidewall, shown in Figure 2.12. The construction seen in Figure 2.12 allows gaps between the strips to be kept to a minimum. Other than that, it is still bound by cable in the same manner as its predecessors (Crook).

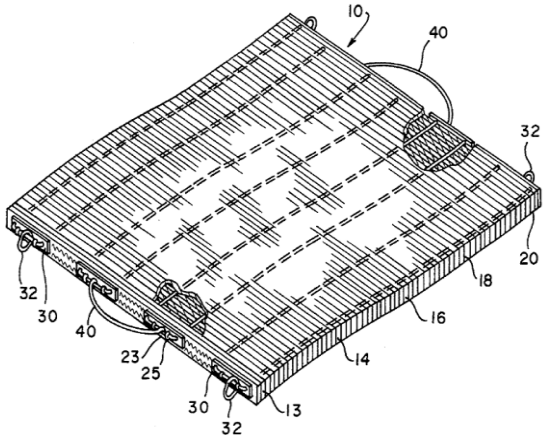

Figure 2.12 Crook Mat Design

2.2. DESIGN ELEMENTS FROM PATENTS

Each of the blasting mat designs examined in this review provide unique elements for mat construction. With the addition of each element there is a trade-off in functionality. Some of the early designs varied widely between each other, but as time progressed, their differences became smaller by new designs blending distinguishing elements. The best example is the sidewall ring mat developed by Goldberg. It uses the sidewall rings of the tires similar to Arcand but fashions the mat in a configuration like Berg's wire-ring mat layout. The design elements discussed in this section are binding methods, material orientation, and constituent materials.

2.2.1. Bindings. Belanger's design as well as those from Lewis, Robertson and King, and Crook all use recycled, worn out, and used rubber tires to protect their bindings from damage as well as add weight to the mats. The result is a more resilient blasting mat that can withstand stronger blasts. The main downfall of each of these designs is the method of binding. Long cables are used to string together small pieces of tread. These cables are the most critical part of the mat. If they are broken or severed in any way, the mat will unravel due to the blast or by equipment moving the mat. With these designs, there are often only two cable intersections per tire section and they can even be the same cable looped back on itself. Such cables are susceptible to failure due to corrosion, excessive pulling and stretching from a blast or equipment, severance in the event of debris penetration, or a combination of these. The cables are the most rigid, inelastic part of the mat. This also makes their failure the most influential in the disintegration of the blasting mat. In spite of this, steel cables are still the most common and durable binder available.

Other methods of binding include using strips of tire material tied in a square knot, such as Goldberg's method, or by using bolts per Meagher's design. The tire material method is the most elastic of the binding methods and allows for a large amount of flexibility, but cannot handle as much tension as the steel cables. The opposite is true for the bolts in Meagher's modular block mat. The bolts keep the blocks that comprise the mat together. They will have more problems from shear stresses generated from block movement due to block rigidity. These bolts are not designed for bending. Excessive bending can quickly fatigue the bolts and cause failure.

2.2.2. Material Orientation. Many of the designs similar to Belanger's rely upon the strength of the mat material as it lays stacked alongside more of the same. Tires, blocks, and plates are all oriented on edge to obtain more bulk and protection for the binder cables and obtain a heavier mat per square foot. This also allows less binding material to be used in relation to the amount of matting. Metal cable and fasteners are the most costly elements of a blasting mat, so reducing them helps save money. Other designs examined were woven or bolted mats. The woven mats have the same reliance of a small number of cables comprising the mat. The device will be prone to unravel in the event of a cable breaking. The bolted block design produced by Meagher is a very rigid mat. From the patent it looks very sturdy and solid. This mat could be likely to act as a larger block rather than flex and conform to the blast as those bound with cables would.

Mail or interlocking ring patterns were also used. These designs distribute forces around the rings, preventing one single element from taking most of the force. This eliminates the possibility of complete failure of the device due to an individual failure. They are easily maintained since the components can be accessed and replaced without undoing the entire mat. The drawbacks to these configurations are the large apertures in between and within the rings, as well as the light weight of the components that make the rings. The large holes in these mats have a higher maximum particle size that can potentially be projected through the mat and off the blast site.

2.2.3. Summary of Design Elements. From the previous discussion, it is obvious that there are significant advantages to certain types of materials and bindings. These are listed as follows:

- A continuous mat material of sufficient strength ensures that particles cannot escape through the mat.
- The size of gaps in discontinuous sections of the mat must be kept to a minimum.
- A mat that does not rely on a single element or just a couple of binders will be easier to repair when a material failure does occur.
- Lightweight components in a mat mean more than one mat will probably need to be used to ensure there is enough mass to resist flyrock material.
- Strong but flexible binders that can bend, but not stretch to a large degree need to be used.

These items were considered for use when designing the form of the blasting mat composed of rubber tractor treads described and tested in this thesis.

The next section discusses the establishment of a standardized test to assess blasting mat performance. The previous work and theory used to design a test for assessing blasting mats is in the next section because it leads directly into, and is an integral part of, the initial estimates of blasting forces.

3. FLYROCK TEST DEVELOPMENT

3.1 NEED FOR FLYROCK QUANTIFICATION

For a blasting mat to be considered functional, it must satisfy two criteria. The first criterion is that the mat can stop all fragments from leaving the blast site. The second criterion is that the mat itself cannot leave the blast site, sometimes easier said than done. Before using a blasting mat in the field, it should be subjected to a standardized test that simulates the rigors of a blast encountered in the field in a controlled non-production environment so that any unintended result does not put personnel, bystanders, equipment or property at risk of damage or injury. Then the mat should be compared to other designs currently in use to determine if it is an equal or more appropriate application than current methods.

A blasting mat's purpose in the mining and construction industry is to stop flyrock. For a feasibility study on blasting mat effectiveness to be valid, the flyrock needs to be representative of what can occur on an actual blasting site. It follows that a standardized test must be developed so that the performance of the new blasting mats can be measured and compared to an industry adopted mat. The initial speed and density of the rock, as well as the volume of the crater left behind can be used to estimate the amount of energy the mats must stop. An estimation of flyrock projection can also be estimated to give an indication of the level of hazard mitigation required.

3.2 FLYROCK ESTIMATION

To devise a standardized test for blasting mats, conditions at the borehole collar and an estimation of the potential hazard are needed to establish the feasibility of a new blasting mat material and complimentary design as well as provide data for comparisons with existing mat materials and designs. The forces created at the blast surface in the vicinity of the borehole can be estimated using rock density, crater volume, and initial velocity. These can be combined to provide the inertial energy encountered by the blasting mat. The calculated energy at the collar of the blast hole can be used to provide a baseline for comparisons of the energy blasting mats will encounter. While these estimations are useful, they are only accurate to a certain degree, and even then multiple

assumptions need to be taken to have a functional flyrock model. Regardless, the model is established starting with the major components, and their explanation. It is first described theoretically and then with values.

The model developed in this work is divided in two portions. Half of the model pertains to the total energy of rock particles leaving the borehole. This is the amount that the mats will need to contain during testing. The other half is an estimation of the hazard encountered from flyrock produced as a result of the blast. Some of the major components are not exclusive to one half of the model or the other and are closely related. These estimations were made for determining the suitability of the test shots, but are not necessarily an accurate prediction of such. The model is based upon the assumption that flyrock produced from a crater blast event will produce a higher flyrock hazard than that of a normal bench blast due to the larger amount of vertical projection. A crater event is also assumed because the blasting mats this project are intended to test sit on top of a shot to stop flyrock. This is representative of a trench or other confined shot, whereas a bench blast would most likely project the majority of it's flyrock from the vertical face. A single blasthole test is used because it has an equal burden in all horizontal directions, where a second borehole would blast to the path of least resistance if placed adjacent to a previously shot hole. This presents a worst case scenario for flyrock, which is what blasting mats are used to mitigate.

Fragment size is based on a mean size estimation. This thesis does not account for larger, slower particles, or smaller, faster particles, but the average energy imparted to the rock at the borehole collar during the blast event. Flyrock size is the first component used in estimating the energy imparted to the rock to create a crater.

3.2.1. Flyrock Size. The first item to determine the estimation of flyrock conditions is the mean size of fragments leaving vicinity of the blasthole. Since the type and amount of explosives used in a blasthole can only impart a finite amount of energy into the surrounding rock, there will be a specific fragmentation produced based on the rock conditions. V. M. Kuznetzov, in his study, "Mean Diameter of Rock Fragments," conducted a series of tests where he shot single blastholes and measured the average size of the fragments produced based on the rock conditions and amount of explosives used. Kuznetzov wanted to find out roughly what size of particles were generated when charge

sizes and crater volumes varied (Kuznetzov, 1973). Equation 1 is the equation Kuznetzov formed based on the testing he conducted.

$$< x > = A\left(\frac{Vo}{Q}\right)^{4/5} * Q^{\left(\frac{1}{6}\right)} \quad (1)$$

Where:

< x > = mean fragment size (cm)

A = correction factor; assume 7 for medium hard rocks

Vo = volume of blasted rock (m^3)

Q = TNT equivalent of the explosives weight (kg)

This equation is very simple. There are only two variables that need to be accounted for, while the "A" is a correction factor based on the quality of rock conditions. Kuznetzov assumes a value of 7 for medium-hard rocks. This is the correction value he used for the limestone formations blasted in his study and was used in this work as well. There is a difference between Kuznetzov's work and the testing done for this projcet. Kuznetzov used charges that were assumed to be spherical. This is a charge with a length to diameter ratio of 6 or less according to the ISEE Blaster's Handbook. However, using a charge with a length to diameter ratio less than 6 is not representative of the blasting procedures used when trenching. Column charges were used during this thesis because they are the same configuration of charges used in most blasting operations. For the sake of this endeavor, the charges are considered the same.

The TNT equivalent charge is needed to scale the power of the explosives. Energy comparison information is available along with current explosives brochures, but they often reference the explosives to ANFO because of its wide use. In Paul Cooper's "Explosives Engineering" (Cooper, 1996), Cooper describes a simple estimate for TNT Equivalency. This is done by taking the theoretical energy content of the explosives in question and dividing it by the theoretical energy content of TNT. The result is the following equation:

TNT Equivalency = E (Exp) / E (TNT) (2)

Where:

E = Theoretical energy of explosive (cal/g) (Cooper, 1996)

This will provide a rough estimate as to the amount of equivalent energy per lb.

The formula in equation 1 is used to calculate the average sized piece of flyrock that is generated during blasting. Kuznetzov's equation still needed a crater volume to estimate particle size. The next section describes the estimation of crater volume.

3.2.2. Scaled Crater Volume. As mentioned in Section 3.2.1, there is only a finite amount of energy that can be imparted into a rock mass by a given amount of explosives. Because of this, there must be a relation between the amount of explosives used and how large of a crater is developed. Julius Roth in his 1979 report to the U.S. Bureau of Mines established a means for estimating just that. While most of the report is based on flyrock generated from bench blasting, Roth has a chapter based on crater generated flyrock and how to determine the amount of flyrock a particular amount of explosives will create (Roth, 1979). The two important terms regarding this work are scaled crater volume (SCV) and scaled depth of burial (SDOB). Scaled depth of burial is a means of comparing different blasthole designs and being able to compare their performance based on physical characteristics such as blasthole dimensions and explosives content. It is calculated first. The ISEE Handbook gives the equation for finding scaled depth of burial using United States standard units as

$$SDOB_{U.S.} = \frac{Is + 0.042 * m * d}{0.305 * (m * d^3 * \rho e)^{0.333}} \quad (3)$$

Where:

$SDOB_{U.S.}$ = U.S. Scaled depth of burial (feet/pound^3)

I_s = Stemming length (feet)

d = Blasthole diameter (inches)

m = Contributing charge length factor

ρ_e = Explosive density (grams/centimeter^3) (ISEE, 2011)

The contributing charge length factor is

$$m_{U.S.} = \frac{12*Ic}{d} \quad (4)$$

Where:

$m_{U.S.}$ = Contributing (US) charge length factor (blasthole diameters)

I_c = Charge length (feet)

d = Blasthole diameter (inches) (ISEE, 2011)

The benefit of using SDOB equations 3 and 4 is that TNT equivalent charges do not need to be calculated to use them. They take explosives into account based on charge density, length and borehole diameter. Stemming length is also accounted for, so this covers all the basic dimensions included in borehole design. When similar scaled depths of burial are obtained, the blasts can be expected to perform the same way, regardless of their size. In comparison SCV is used to estimate performance.

SCV is the size of a crater formed by a blast performed at a given SDOB. The SCV is multiplied by the amount of explosives used to give the total expected volume of a blast. Roth plotted the crater volume for sandstone and granite based off SDOB. This gave a rough estimate of crater volume that would scale with charge weight and depth. Since Roth's study created a scaled model, it could be applied to smaller borehole designs than those used in Roth's study. Figure 3.1 is Roth's plot for SCV. The top curve is for sandstone, and the bottom line represents granite. These curves are used to estimate the SCV. SCV is the volume of crater produced per pound of explosives. It is multiplied by the amount of explosives used to produce a crater volume. Since the MST Experimental Mine has mostly limestone and contains no granite or sandstone for blasting, the value for limestone was assumed to be similar to that of sandstone for the purposes of this estimation. (Roth, 1979)

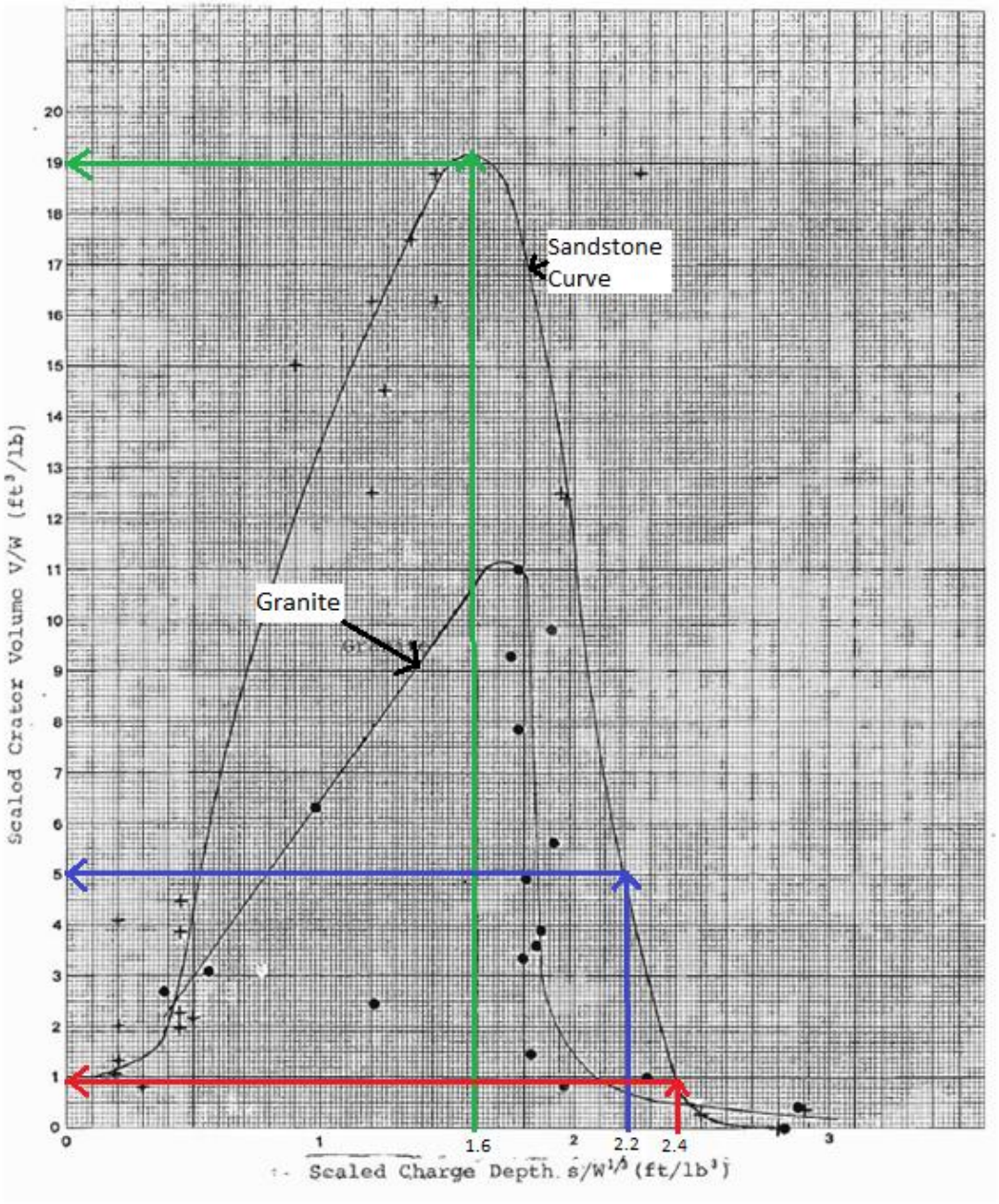

Figure 3.1 Scaled Depth of Burial vs. Scaled Crater Volume (Roth, 1979)

3.2.3. Fragment Ejection Velocity. Fragment ejection velocity is needed in conjunction with density and crater volume to determine the muzzle energy at the collar of a borehole. This is needed when comparing performances of blasting mats because it

gives a quantitative result that can be scaled or used as a standard. When combined with the mean particle size and density, the resultant can also be used to determine the energy contained in the average piece of flyrock.

Roth observed and plotted flyrock velocities based on SDOB, but the data points are scattered and the trend line is loosely approximated. The ISEE Blaster's Handbook contains an equation, from A.A. Chernovskii in 1985 that can be used in estimating the initial projection velocity of particles. The equation from the handbook is based on particle size, density, and borehole diameter. It does not account for SDOB but is an estimated maximum initial velocity [*There was some skepticism from the committee concerning this equation because it looks unfounded. There are many items in the current edition of the ISEE Handbook that are wrong. However, the problems associated with the application of this equation are discussed in Section 3.5.2*]. The ISEE Blaster's Handbook does not state whether this equation can account for stemmed or unstemmed holes, or whether SDOB is a factor, but as it describes a worst case velocity, the assumption is that it was adequate for this study. This equation does not account for explosives weight, velocity of detonation, or chemical structure of the explosive used. It is simply an approximation. Worst case projection velocity is estimated using Equation 5.

$$Vo = 10\,(d/\,x_f) * (2600/\,\rho_r) \qquad (5)$$

Where:

Vo = initial projection velocity (meters/second)

d = diameter of borehole (inches)

x_f = fragment size (meters)

ρ_r = rock density (kilograms/meter^3) (ISEE, 2011)

With this estimation, initial flyrock attributes can be approximated, and this information can be carried on to the next step of estimating flyrock projection.

3.2.4. Flyrock Range. The ISEE Blaster's Handbook also has many other useful tools available for explosives engineers to use in the design and estimation of blasting results. The next item used in flyrock estimation is taken from this handbook. The reason for this is that the Handbook contains work that estimates the trajectory of

flyrock pieces, rather than finding a maximum flight distance and establishing safe blasting boundaries based off of those estimations. The Handbook contains other versions of these methods as well, but estimating average flight distance is more useful for this laboratory setup as it gives a practical estimation of where rock will be during any given time after launch. It also provides a worst case flight path for an average piece of flyrock. This estimation uses two equations solved simultaneously. Equation 6 gives the projection distance along the initial angle of projection with respect to time, and Equation 7 provides the amount of drop from this line with respect to time. Equation 8 is a factor that allows equations 6 and 7 to account for the mass of flyrock particles (ISEE, 2011).

$$Z = (1/b_d)*\ln(1+b_d V_o t) \quad (6)$$

$$Y=(1/b_d)*\ln ((\ e \wedge (\ 2*t*\sqrt{(\ b_d*g))+1) / (\ 2 * e \wedge (\ t * \sqrt{(\ b_d * g\ )}\ ) \quad (7)$$

$$b_d=1.3/(x_f*\rho_r) \quad (8)$$

Where:

V_o = Projection Velocity (meters/second)

t = Time after launch of the fragment (seconds)

g = Acceleration due to gravity (9.81 meters/second^2)

x_f = Fragment Size (meters)

ρ_r = Rock density (kilograms/meter^3)

Z = Distance measured along the line of the initial projection angle (meters)

Y = Vertical distance measured from the line of initial projection (meters) (ISEE, 2011)

An initial angle of projection, α, is assumed because these equations do not specify one. In Roth's flyrock observations, 45 degrees from horizontal is the angle that provides the furthest projection. From here equations 6 and 7 are solved simultaneously using Microsoft Excel's Solver function. The vectors calculated will meet and produce a right triangle at the point where the particle hits the ground. The actual path of the flyrock

is an arc, but assuming that the rock lands at the same elevation, a triangle with x as the horizontal, y as the vertical, and z as the hypotenuse is produced. This total horizontal distance traveled by the fragment can them be determined by solving for the cosine of the resulting triangle. Figure 3.2 is a representation of the path traveled by a fragment, and the vectors produced by these calculations. This is the last component of the estimation and although it does not influence energy estimations, it provides a sense of scale that allows potential hazards to be easily visualized.

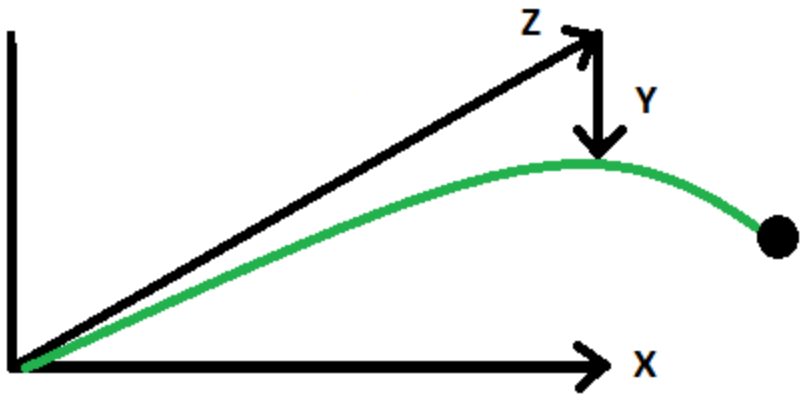

Figure 3.2 Projected Fragment Path

3.3 SELECTION OF VALUES

In the previous section, a theoretical model was created to estimate flyrock conditions near the blast hole. At this point realistic values must be inserted into the model to obtain the flyrock estimates. These values must represent a small scale blast that is likely to cause damage to property or equipment in close proximity, but still be manageable with conventional blast mat application. Most often this is related to blasting trenches in urban areas for utilities to be installed. These blasts can be placed close to houses and other property since the trenches created will later contain water, sewer, or electrical utility lines. They are typically long single or double row blast patterns using shallow, small diameter boreholes, shot in a slow sequence from end to end. From

personal observation, places along a trench shot where flyrock becomes an issue are the initiated ends of the trenches and places where misfires have occurred. In both instances, the confinement around the next borehole due to solid ground conditions causes more blast energy to be directed to the top of the borehole instead of out into the area of broken rock that would be adjacent to it. With the energy directed upward, broken rock is projected higher than if the confinement was not there. This assumption simplifies the blasting mat test to a single-borehole cratering design similar to the test setup shot by Kuznetzov (Kuznetzov, 1973).

3.3.1. Blasthole Depth. For testing the blasting mat, the blastholes were sized according to their potential application. A utility trenching application was assumed. In trenching, the depth of the blastholes is dependent on the type of utilities to be installed. According to Rolla Municipal Utilities, primary electric lines are generally buried 4-6’ in depth and water lines are buried 4’ deep to remain below the frost line to prevent damage to those utility lines during winter and spring frosts. Trenches are dug another 1’ beyond that to ensure there is room to work around the pipe and install bedding material for the pipe to rest on (Cason, 2012). To ensure breakage to the 5’ mark, it is normal to add an additional 1’ of subdrill, bringing the total depth for each blasthole to 6’. This depth was held constant for all testing associated with this project as it was a practical representation of appropriate borehole length.

3.3.2. Explosives Selection and Blasthole Diameter. The selection of explosives was the next step in blast design. With 6' deep holes, care had to be taken to ensure that the explosive product used was reasonably sized and applicable for a small trenching job. Due to the hypothetical close proximity to buildings and other properties that could be damaged, the overall charge weight per delay needs to be kept low, but still have enough energy to thoroughly break the rock. Another required consideration is the ability to load consecutive holes consistently. Often times when drilling is conducted, the actual inner diameter of the borehole will vary along its length. Mud seams, voids, weak spots and jointing effects can cause the drill bit to deviate or remove more material than anticipated from parts of the borehole. Sometimes these can be estimated by the driller, but they are often unaccounted for. With short length, small diameter boreholes, the changes in volume are typically much smaller, but using bulk explosives such as ANFO, emulsions,

or a blend would still have inconsistent loading results. By using cartridge explosives, the total amount loaded in the hole can be kept consistent and uniform. In addition, cartridge explosives are convenient for small blast designs because they can be loaded quickly and counted easily. They do not couple with the borehole as well as bulk systems, but this allows the same amount to be placed in consecutive boreholes regardless, as long as no large voids are present.

The Explosives Engineers' Guide, published by Dyno Nobel, is a brochure that contains the different types of explosives available for use from Dyno Nobel, as well as information on their properties and applications. Unimax nitroglycerine dynamite was selected from this pamphlet as the explosive for blasting mat testing. It is a high strength dynamite, often used in trenching, that functions well at smaller diameters, with an explosive density of 1.55g/cc (Dyno Nobel Inc, 2003). A common size of 1 1/4" x 8" sticks was selected, with each stick weighing about 0.4lb/stick. They were paired with Unidet 25/350ms nonelectric blasting caps, commonly used in trenching, that were donated by Buckley Powder Co, a distributor and shot-service company for Dyno Nobel. Buckley donated the dynamite and nonelectric caps, as well as electric blasting caps to be used as starter caps. 1.5” diameter holes were selected for this application because they allow easy insertion of explosives cartridges and still have a high volumetric utilization. Holes of this diameter can be easily drilled by various sizes of pneumatic drills. Brunner and Lay donated a 1 1/2" bit and 8' drill steel for the Experimental Mine's air-track drill to be used for this testing. In commercial blasting operations, cartridge explosives are often tamped into the borehole to ensure that they stay put, as well as to improve the overall use of the borehole volume. The degree of tamping that the cartridges allowed was measured to determine the loading density.

The amount that the dynamite shortens when tamped in a borehole was measured using a 1.5” diameter section of PVC pipe. A stick of the dynamite was tamped into the pipe and reduced the length of the stick from 8” to 6”. This provided a basis for estimating the amount of dynamite needed to obtain the tamped powder column heights.

3.4 TEST VARIABLES

The objectives of this first series of tests were to measure the amount of flyrock that could be generated at that location with the current design and obtain consistent results in amount and initial velocity of rock fragments. A practical maximum of flyrock generation gives a harsh but fair scenario of what a blasting mat must endure. Evaluating flyrock conditions without mats is essential to understanding the actual behavior of the mats.

Powder column height and degree of tamping were the two variables that were changed during the first set of tests. By varying the height of explosives, the net weight of explosives in the borehole increased. The explosives weight was further increased on holes that were tamped. This packed as much explosives in the holes as possible for a given powder column height. The increase in height of the powder column reduced the burden of the shot by lowering the SDOB. Holes loaded with smaller powder column heights had more rock on top of them to potentially throw, but had less energy to impart into that rock. With higher powder column heights, the smaller amount of overlying rock could receive more of the imparted energy and potentially throw those fragments faster. Powder column heights tested were 3', 4', and 5'. Five feet was selected as the maximum to allow at least 1' of stemming material to contain some of the energy around the mouth of the borehole. This was an experience based maximum value because loading a borehole to the collar in this case would be an irresponsible practice, and throw off an attempt at SDOB calculations. Figure 3.3 is a diagram showing the different loading configurations that were used during the flyrock testing.

Testing was ordered starting with the 3' powder column tests and then incrementally increased to ensure that any excessive flyrock conditions created during the testing would not put students or workers elsewhere on the MST Experimental Mine property in danger. Changing degrees of tamping changed the amount of explosives at the given powder column height. Each powder column height was ordered so the un-tamped condition would be tested first. This was for safety as well. The effects of the better charge coupling with the sidewalls of the borehole as well as the overall increased weight in the hole could put people at risk. To ensure that equal amounts of explosives were going in the holes, the explosives were counted out beforehand and put to one side to

avoid mistakes. Un-tamped holes were loaded with the amount of dynamite that resulted in the desired powder column height with loose sticks. For 3’ holes, this was 4.5 sticks, for 4’ holes, this was 6 sticks, and for 5’ holes, 7.5 sticks. Tamped holes were a different matter. The initial cartridge that held the blasting cap was inserted into the borehole without tamping. Tamping this primed cartridge could result in unintended initiation with personnel in the blast zone and is prohibited by regulations. The additional cartridges were slit and tamped. Slit and tamped cartridges are less likely to flow into small crevices than bulk systems, which might have caused unwanted variations in the loading profile. Explosives amounts were allocated before loading the tamped holes as well to avoid mistakes. Explosives were measured to the nearest ½ stick. Tamped holes received 5.5, 7.5, and 9.5 sticks of dynamite for 3’, 4’, and 5’ powder columns respectively. Each stick was tamped, with the exception of the primed cartridge, so the packing of the powder column was even throughout the borehole except at the primer location. Once the holes were loaded, they were stemmed to the top with 3/8” river rock on hand as described in Section 5.1.4.

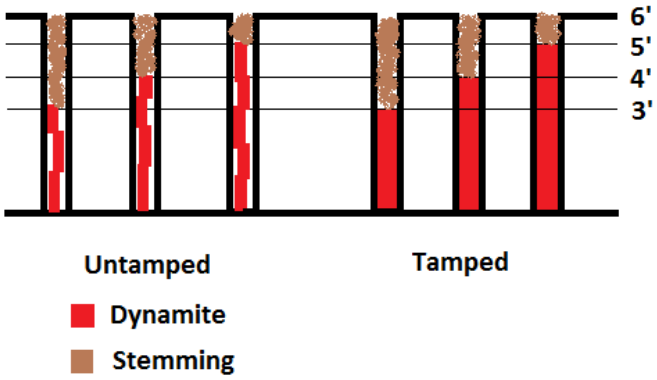

Figure 3.3 Flyrock Test Loading Configuration

3.5 ESTIMATION OF FLYROCK FOR INSTRUMENTATION SETUP

With the selection of the variables in the shot design complete, their chosen values were placed back into the previous estimation formulas to form the model that would determine equipment and settings for estimating flyrock conditions. The first portion of the estimation was be an energy estimation, and the second part was a hazard indication. Some of the components were used in estimating both. Care had to be taken because of the mixed metric and US units.

3.5.1. Estimated Crater Volumes. The first step in muzzle energy estimation is crater size. This is readily estimated using Roth's chart to find SCV and multiply it by the charge weight. To use this, the SDOB must be determined. A minimum and maximum value were determined based on the extremes for powder column height and charge weight as previously determined. This was done using Equations 3 and 4. Because the charted reference material is in U.S. units, SDOB must be calculated in the same units. Using the values from Section 3.3, these equations are simple fill-in calculations. Table 3.1 contains the estimations for the flyrock model for estimated crater volume as well as the other calculated aspects of the estimation. Where U.S.-metric conversions are required, the Android application ConvertPad was used to get equivalent values. A sample calculations for these estimations is available in Appendix A.

This model is used for estimation and requires some common sense when interpreting the results. SDOB is the first component and influences the remaining components. The SDOB value that produces the largest crater volume is going to be around 1.6ft/lb^3 for most rock types. A SDOB value lower than that will result in a smaller crater size because the charge is not contained by as much stemming material. When the SDOB is higher than 1.6ft/lb^3, the charge is being buried deeper, reducing crater size. The scaled depth of burial values for the minimum and maximum test size are 2.97 and 1.95 respectively. Both of these values are representative of the real world conditions. Even though the maximum charge weight was loaded almost to the top, the charge weight was kept small, which made for a higher than optimal SDOB.

Table 3.1 Initial Theoretical Flyrock Values

	Minimum	Maximum
Estimated Crater Volume		
Charge length factor (Eqn 4)	24	40
SDOB (Eqn 3)	2.97	2.23
Scaled Crater Volume (Fig 4.1)	0.3	5
Estimated Crater Volume (ft3)	0.675	23.75
Mean Fragment Size		
TNT Equivalent Charge kg (Eqn 2)	0.79	2
Mean Fragment Size cm (Eqn 1)	0.31	3.27
Initial Velocity		
Initial Projection Velocity m/s (Eqn 5)	4914	466
Flyrock Projection		
Z (Eqn 6) (m)	51	266
Y (Eqn 7) (m)	36	188
α	45	45
X (m)	36	188
Initial Energy ft lbs	870600	2295300

3.5.2. Mean Fragment Size. Mean fragment size is used as the basis for for velocity estimations. This is where some interpretation must be used to obtain useful estimates. Table 3.1 contains the results of the mean fragment size based on the estimated crater volume from SDOB and Roth. These numbers are a severe underestimate on the size of the rock fragments. Roth states that with current velocity estimation methods based on his plotted curves, they are difficult to follow if the curves are used past their maximum. This leads to overly large launch velocities (Roth, 1979). The point in these calculations where problems occur is in determining mean fragment size. Kuznetzov's method is based on charge weight compared to crater volume. This is most accurate near the maximum of the SDOB vs. SCV curve. With lower SDOB values, crater volume does decrease, but the amount of energy available for rock breakage in the upper areas of the

powder column is larger. SDOB indicates that this will lead to smaller craters, possibly due to the close proximity of the surface. As SDOB increases to its maximum, there will be larger fragments because stemming will cause the energy to spread out among the rock mass further. This will result in larger fragments, resulting in lower launch velocities. Once the maximum SCV is reached, further increasing the SDOB lowers the efficiency of the shot (Roth, 1979).

According to the model, if the scaled crater volume starts to decrease because the SDOB is above 1.6ft/lb^3, Kuznetzov's equation causes fragment-size to decreases. With smaller particle sizes, launch velocity from equation 5 increases rapidly. In reality, larger SDOBs, above 1.6ft/lb^3, will cause the shot to throw less rock and will not break as well. It is at this point in the calculations that mean fragment size must be calculated under the assumption that it is at the maximum SCV. In reality, high SDOBs will have a lower launch velocity than those with a SDOB of 1.6ft/lb^3 or lower. The model does not account for this, so the mean fragment sizes must be calculated using the maximum crater volume. Any attempts at calculating actual values past optimal SDOB with this model will result in a great underestimation of fragment size, and as a result, an overly large initial velocity like those in Table 3.1. The model was re-worked using the maximum scaled crater volume. Table 3.2 shows these calculated values.

The initial projection velocity shown here is the upper limit for the test shots. It is unknown how much of an overestimation this is, so a conservative testing regimen was needed, shooting the lowest risk charges first and working up.

3.5.3. Initial Projection Velocity and Trajectory. Initial projection velocity and trajectory are at the end of this model as far as calculations are concerned. Being dependant on the previous overestimate calculations, these estimations will also yield above normal results. The initial velocity of flyrock particles was measured with a Phantom V10 high-speed camera during actual testing, and then the model was adjusted so that it is representative of reality. The initial energy estimation, shown at the bottoms of Tables 3.1 and 3.2 was used to compare the energy input from the different tests. Since the model was assumed to have an even velocity distribution over the projected particles, the velocity component of the energy estimations was halved to represent a mean velocity. This mean velocity combined with the weight of the rock that would fill the

crater provided the estimate for energy that a blasting mat would have to stop for these tests. These initial values were based on assumptions and compared to real values when test data was examined.

Table 3.2 Adjusted Theoretical Estimations

	Overestimate
Estimated Crater Volume	
Charge length factor (Eqn 4)	40
SDOB (Eqn 3)	2.23
Scaled Crater Volume (F 4.1)	19
Estimated Crater Volume (ft3)	72.2
Mean Fragment Size	
TNT Equivalent Charge (Eqn 2)	2
Mean Fragment Size (Eqn 1)	8.81
Initial Velocity	
Initial Projection Velocity m/s (Eqn 3)	170
Flyrock Projection	
Z (Eqn 6) (m)	417
Y (Eqn 7) (m)	295
α	45
X (m)	295
Initial Energy ft lbs	3245300

3.6 THE COMPLETED MODEL

At this point, the flyrock model was as complete as it could be until testing could provide actual flyrock data. It was in an assumed worst case scenario for flyrock conditions with calculated values above what the author's experience indicated. The size and velocity estimates in Table 3.1, and the estimated crater volume of Table 3.2, were not representative of the test shot parameters that were used in the flyrock tests shown in Tables 5.1 and 5.2, discussed later. Since all the test scenarios had scaled depths of burial

well above the peak scaled crater volume, this model needed to be adjusted so future estimations would be more representative. With the model expressing an outer boundary for flyrock conditions, blasting and observational equipment was selected, and flyrock conditions evaluated.

4. TRACTOR TREAD MAT DESIGN

4.1 TRACTOR TREAD MATERIAL

The four pairs of rubber tractor treads were donated by Kolb Grading. The treads, manufactured by Camoplast, consist of 1/4" steel cables running lengthwise in parallel continuous loops, crossed with 1/8" steel cables spanning the tread's width. These cables provide much of the tensile strength for the tread. The cables are encased in vulcanized rubber, which provides the bearing surface and keeps the cables together. Tracks are molded onto the outside of the tread loop to provide traction between the machinery and the ground, while cleats are molded to the inside of the loop to allow the machine to move on the treads as in Figure 4.1. The result is a tractor tread ranging 2.5-3.5' wide, 20-24' in length or circumference, and 2.5-4" thick. These are general measurements as the treads are manufactured for specific models of machinery, not one size fits all. Figure 4.2 shows one of the treads donated by Kolb Grading. The size of the tread shown in the picture was 32" in width, 20' in length or circumference, and 2.5" thick with an additional 1.5" high cleats, highlighted in green in Figure 4.2. Treads of this same size were used for testing in this thesis.

Figure 4.1 Tractor Treads on John Deer Mobile Equipment (Mascus)

Figure 4.2 Rubber Tractor Tread

4.2 ASSEMBLING THE BLASTING MAT

4.2.1. Introduction. The rubber tractor treads were found to be extremely resilient. The strength of these treads made them good candidates for blasting mats. They were difficult to cut or puncture, which was a benefit when they were being used as a blasting mat, but made things more difficult during the mat's construction. The difficulties of cutting and puncturing the treads, and their associated solutions, are described in the following sections.

4.2.2. Cutting the Treads. When the treads arrived at the MST Experimental Mine, they were still in complete loops as they were when they came off the mobile equipment. Four pairs of these treads showed up to the mine. The treads delivered were 20' in circumference, like the one pictured in Figure 4.2. These treads needed to be cut into strips to assemble into the blasting mat.

The treads are extremely robust and presented a challenge. Multiple methods were tried to cut these treads. The first assumption that was made was that the treads could be cut with a reciprocating saw with a steel-cutting blade attached. This method was successful in cutting the treads but it took multiple saw blades and several hours to accomplish this task. The amount of time it took to produce a cut was partially due to the ductile and flexible nature of the treads. The steel and rubber flexes, stretches, and

moves with the motion of the saw, absorbing most of the energy. The saw batteries had to be changed at least four times during the course of one cut and the process was very taxing for the saw. This method is very costly due to the usage of multiple blades, wear on equipment, and the man-hours required producing the cuts.

The second attempt to cut this material involved a large gasoline powered circular concrete saw that is used to cut grooves into sidewalks and concrete foundations. This was expected to be marked improvement. However, it was a complete failure. The saw was unable to complete a cut and created a lot of smoke from the friction between the blade and the treads. The saw cut slowly for a few inches and then stopped completely. The friction from the rubber on the large surface area of the blade was enough to stop the saw blade.

The next attempt to cut the treads used a hydraulic shear to slice the rubber and steel tread apart. The Rolla City Fire Department brought their "Jaws of Life," a portable hydraulic shear, out to the Experimental Mine to see if they could cut it, which would give them more practice with the tool as well. This method was a failure as well. After an hour and a half, the shears only removed a small triangular notch from the edge of the treads about 3" wide and 3" into the treads. The shears, although powerful, were only made to handle small amounts of sheet metal, such as pillars and door latches on an automobile. This application was too strong for both the shear jaws and the hydraulic pump that powered it. A large shear on demolition equipment is required to have enough strength for that method of cutting to be viable.

After the previous attempts, it was apparent that a more aggressive mindset was needed to sever these treads. The ductile nature of the material made it deform as it was being cut, so a solution that allowed little deformation and had a high enough energy input was needed. Linear shaped charges, used in the demolition industry for cutting applications, provide overwhelming power to ensure that their targets are sliced clean through. These shaped charges create blades that travel fast enough that the target material would not have enough time to deform. These were the answer to the tread cutting problems. For this purpose, short end-lengths of 600gr./ft. linear shaped charges were used, donated to the MST Explosives program by Dykon Demolition. These end-sections of shaped charges had been cut off of a longer piece of shaped charge and not

used because the ends were crimped and deformed when they were manufactured, or explosives had fallen out of the ends and there was a void where powder should be.

Since this application did not require as much precision as a demolition project, the ends of the charges were filled flush with C4, and affixed end to end along a piece of interior molding. This provided rigidity to the pieces and allowed them to function as a longer, single unit rather than individual lengths, shown in Figure 4.3. Each assembled unit had approximately 36" of shaped charge. An 8g "stinger" cast booster was affixed to the end of the assembly to allow for initiation from the blasting cap. Foam pieces of 1" thickness were attached to the blade-producing side of the charge to allow proper stand-off distance for the blade to properly form before it impacted the treads.

Figure 4.3 Composite Linear Shaped Charge, Constructed of Surplus End Pieces

After these shaped charges were assembled, the treads were taken to the quarry area at the MST Experimental mine so they could be cut. The treads were placed on the ground, with the equipment-bearing side facing up. This was to ensure that the charge on top was placed so it would cut through the cables first if the charge weight was insufficient to cut through the entire material. The charge was laid across the width of the

tread and initiated. The tread had a clean, straight cut across its entire width. This result is a straighter and less ragged cut than the one produced by the reciprocating saw. For our operation the linear shaped charges were the cost effective solution to cutting the treads.

Using 600gr./ft. linear shaped charge for this type of cutting was also an efficient use of explosives in that nearly all the blades that cut the treads were recovered from the ground beneath the mat, having penetrated only an inch or two. This meant most of the energy from the blades was put into the treads, but enough was left over to ensure a complete cut. From a time perspective this was also beneficial because assembling, placing, and shooting one of these charges took about 15 minutes at our operation. This was the easiest and fastest way to cut the rubber tractor treads. It also produced a cleaner cut than the other methods mentioned.

4.2.3. Puncturing the Treads. With the treads cut into appropriate lengths, the next step in producing a blasting mat was to puncture the treads so that cables or bolts could bind them together. The width of the treads, compared to their thickness made it obvious that it would be very impractical to punch holes in them in any other orientation than normal to their bearing surface. Some of the designs described in chapter 2 have holes for fasteners in the same direction through their materials.

As with the attempts to cut the treads, mechanical methods were tried to bore through the treads to provide clean holes for the fasteners to run through. A 1" diameter drill bit was used for the first attempt. This was able to bore out the vulcanized rubber but was unable to penetrate the steel cables in any manner, even with the operator's entire bodyweight on the drill. It also produced plenty of black soot from the constant friction and the bit had to be oiled to keep from burning up the drill motor. The rubber that was removed stuck in the grooves of the bit and cooled, making it difficult to clean out. The drill bit could not penetrate the cables, possibly because of its large diameter.

A 1” stepped drill bit was used next to try to bore a hole. These bits are made for metal working because they are hardened and start with a small tip to get a pilot hole started, and the hole can expand from there in increments. However, this attempt did not work either. The bit had the same problem of not being able to penetrate the cables even though the bit was much smaller at the tip.

Since the drill bits could not penetrate the cables, a 1" hole-saw was the next attempted solution. The hole-saw was a viable solution but not an easy one. As with the bit, it had to be oiled and the rubber would clog up the hole-saw. Since the rubber squeezed into the hole-saw, it was difficult to remove. It would take 15 minutes or more to remove the plug of mangled rubber that built up in it. The hole-saw did penetrate the steel cables, though not very efficiently. Rather than a cutting motion seen by using a hole-saw on wood and other more rigid materials, the hole-saw would hook onto the wires in the cables and would twist and tear the wires from the rest of the cable before continuing through the remaining rubber. The wires would become tangled within the hole-saw along with the rubber and would take much longer to clean out than just the rubber. This twisting and tearing would also dull the saw teeth and in some cases snap them off of the rotating cylinder. A hole-saw would usually last through one hole, or if a better quality hole-saw was used, two holes. Replacing these tools for each hole would be costly if a better method was not found.

Taking ideas from the previous cutting trials, an explosive method was devised to penetrate the treads. Conical shaped charges are used by the military and demolition industries to punch holes in resilient materials where conventional cutting methods would be infeasible. They do this by either producing a material slug that travels through the material like a bullet, or by the shape of the explosives itself focusing blast pressures towards the target. Because it didn't make sense to use costly conical shaped charges from a factory or company on a blast mat made out of scrap materials, cheaper, more abundant materials were used to comprise the shaped charges for penetrating the rubber treads. Three different containers were used on a short test piece of tread to see their effects. The conical bottom portion of a wine bottle, containing 6oz. of C-4, with a 2" standoff comprised the first charge. The second charge was the bottom half of an 8.3oz. Red Bull can and (using the parabolic dished bottom to make an Explosively Formed Projectile) contained 2oz. of C-4, with a 2" standoff, shown in Figure 4.4. The third charge was made from a 12oz. Coors Lite can (EFP) with 2oz of C-4, with a 2" standoff. The 2" standoff distance for these charges came from the height of the Dixie Cups they were sitting on.

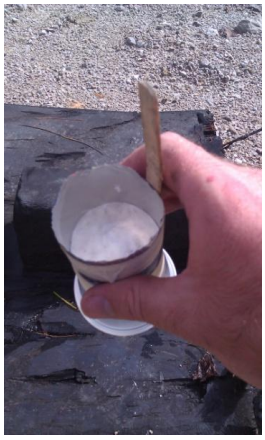

Figure 4.4 Red Bull Shaped Charge

The charges were tested one at a time on the treads, with the treads oriented equipment-side up. All of the charges penetrated the steel cables in the treads. The wine bottle managed to penetrate all the way through the tread and into the ground below. The same with the Red Bull can, although a slightly smaller diameter hole was produced. The Coors can charge did penetrate the steel cables, but did not penetrate clear through the tread. The reduced use of explosives and adequate performance made the Red Bull can charge the best for penetrating the cables in the treads. Even though a hole through the tread was created by the explosive charge, the holes still needed to be bored to a final diameter of 1" to accommodate for the installation of fasteners. Once the cables within the treads were penetrated, they could be easily bored out to the proper diameter with the hole-saw and drill bit discussed earlier.

4.3 MAT DESIGN

When all the holes had been fashioned, it was time to fasten the mat together. The orientation and method of fastening took some thinking. There were previous designs using long flat strips of material for matting and many methods for binding the mats. If the treads were built into a Bellanger style mat of equivalent coverage, the treads would be placed every 4" due to tread thickness. For a 10' by 6' blast mat, eighteen 10' long strips would be needed to comprise the mat. At roughly 420lb per 10' section, this

brought the estimated mat weight to at least 3 3/4 tons without any cables or hardware, which would further increase it. This weight would be excellent for blasting purposes, but attempts to move or place the mat would require very large equipment that would probably not be available at a blast matting operation.

It was not practical to assemble the tractor tread mat like the numerous rubber tire mats with the treads stacked on edge. They could not be tied together or woven like the woven cable and wire-ring mats. A mat weighing in at almost 4 tons would be impractical to move around. But, by rotating the sections until they have the desired overlap distance, the mats can be constructed to a specified weight. Lap joints use a small amount of tread width to allow binding through the overlapping portion. Figure 4.5 shows the lap joints that were used for the tractor tread mats.

Lapping the treads uses more treads to cover the desired width than if they had been laid side by side and fastened in a butt joint configuration. The resulting mat is heavier but does not have places in between fasteners that would become open apertures during a blasting event. The tractor tread blasting mat was constructed with the fastener holes punched about 3” in from the edge. This was so that an overlap of 3” existed on either side of the fastener for a total overlap of 6”. This prevents launched fragments from exiting the mat unhindered. A drawback to this design is that the gaps left between the tread lugs and the next tread are small and directed at 90 degrees horizontal from the direction of the exiting explosives gasses. This added resistance in conjunction with a lightweight construction can possibly cause the mat to become airborne during a blast. If a mat leaves the blast site, it can potentially be more harmful than the smaller rock it would have blocked. Even when mats are used, care must be taken to ensure the immediate area surrounding the blast site is secured.

4.3.1. Fastening the Mat. The treads were strung together using 1’ lengths of 5/8” steel cable and fastened with 3” galvanized washers and ferrule-and-wedge ends. This assembly produced a small cable bolt that pinned two adjacent treads together. The components for each cable bolt are shown in Figure 4.6.

Figure 4.5 Tractor Tread Lap Joints

Figure 4.6 Cable Bolt Components

There were 5 bolts pinning each of the two outer treads to the center for a total of ten cable bolts. This design differs from that of previous designs in that the binding method is the least critical part of the mat. The cable bolts do not run the entire length of the mat and only bind together two of the pieces. Also, if one of the cable bolts were to fail, the entire mat would not fall apart. These bolts were made to be the least important part and to be replaceable. The bolts were threaded through the holes in the treads using a needle made from a piece of metal conduit with the end mashed shut. Inserting the cable into the needle and threading it through kept the cable from fraying and unraveling during installation. Once these bolts were loose-fit, the mat was shuffled around and the bolts tightened to prevent the ferrules from relaxing and falling off. The finished mat is shown in Figure 4.7. This picture shows the mat resting on top of a muck pile. From this view, the tops of the cable bolts can be seen as well as the apertures that occur between the tread cleats from one strip laying atop another.

Figure 4.7 Tractor Tread Mat After Blasting

4.3.2. Finished Mat Comparison. With the completion of the binding and fastening, the mat was finished. The completed mat possesses a modular design that many of its predecessors lack. Like Meagher's modular block mats, this mat can be made to size easily. With only three strips of matting material and ten cable bolts, this design is very simple. Where hundreds of tire strips comprise the Belanger style mats, three strips of matting cover approximately the same area with the tractor treads. Instead of a half dozen cables at least 10' in length to bind the mats, ten 1' cables were used, further reducing materials used as well as making repairs in the field a possibility. It also ensures that the fasteners are independent of one another. This mat weighs in at 1260lbs and covers an area of 10' by 6.5'.

A Belanger style mat of similar size was borrowed from Twehouse Construction Company out of Jefferson City, Missouri. Its manufacturer was unknown. This mat was used as the basis for performance comparison with the tractor tread mat. The Belanger

mat weighed 2360lbs, covering 11.5’ by 6’ in area. These two mats were tested against a standardized blast and their performances compared, as discussed in Section 6, to determine the effectiveness of the tractor tread mat design.

.

5. EQUIPMENT SELECTION AND FLYROCK TESTS

5.1 EQUIPMENT SELECTION

Equipment selection was conducted after the flyrock estimations were completed. The equipment selected for flyrock observations consisted of a Phantom V10 high-speed camera, velocity board, and standard shot cable and blasting box necessary for setting off a blast. This section describes the camera and velocity board setup, loading and test setup, flyrock test results and discussion on those results. The Phantom V10 digital high-speed camera was used to record both the flyrock and blasting mat tests. The Phantom was selected for this testing because it was readily available and had large enough frame rates and memory to capture the flyrock event.

5.1.1 Camera Setup. The Phantom is a high-definition digital camera capable of capturing up to 10,000 frames per second. It was fitted with a Nikon AF Nikkor 50mm wide angle lens with a 1.4 fixed magnification to, at a minimum, capture the whole velocity screen within the picture frame. The only manual adjustments made on the Phantom were adjusting the focus and F-stop on the Nikon lens for distance and lighting conditions. This camera was controlled via a laptop which wrote the video files directly to the hard drive. All the digital camera settings were controlled from this laptop including exposure time, frame rate, and resolution.

The frame rate was the basis for the laptop-controlled camera settings. Frame rate settings were determined based on the estimated ejection speed from the theoretical model in Section 4. The adjusted flyrock model value for initial velocity in Table 3.2 is approximately 170m/s, or about 560ft/s. To ensure that particles traveling through the view of the camera could be captured in at least 2 frames, a frame rate of 2000 frames per second was selected. The exposure time and resolution were maximized once the frame rate was fixed, to increase visibility because of varying lighting conditions due to cloud cover and time of day. A 497.5 microsecond exposure time and a resolution of 980x760 pixels were the maximum allowed values at this frame rate. The large exposure time allowed recording to be done during low lighting conditions such as early morning hours and cloudy weather. These maximum values were used for all testing. The remaining settings for the camera, such as brightness, black and white contrast, and gamma

adjustment (washout) were adjusted on the computer during post processing. The camera was manually triggered for these flyrock tests. The remote trigger was used later, during the blasting mat tests, to eliminate operator error encountered during the flyrock testing.

5.1.2. Camera Protection. Because of the violent nature of the testing and close proximity of the camera, less than 120' from each blast, the camera was placed in a metal enclosure (blasting shelter) with clear plastic viewports to protect it from flyrock. The distance from the enclosure to the blast hole varied from shot to shot, since each new shot had to be conducted in a different place than the previously blasted craters and the same blasting shelter location was used for multiple shots. This shelter was placed in positions where a clear view of the shot could be seen, and as close to the same elevation of the center of the velocity board as possible. By keeping the camera approximately the same elevation as the center of the velocity board, the influence of camera distortion was kept to a minimum. Sometimes this included placing the camera enclosure atop the blast tunnel at the MST quarry. The camera was placed no higher than the top of the velocity board in all but the first 3 tests, described later. A range of errors from distortion is discussed in Section 5.1.3. Figure 5.1 is a photo of the camera and enclosure sitting on the blast tunnel so that elevation differences were minimized. With the camera in place, a scale of reference was needed to allow for measurement of the rock fragments' velocities and is described next.

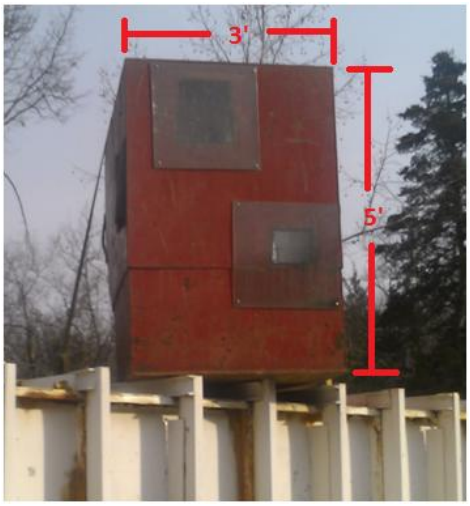

Figure 5.1 Camera Shelter Atop Blast Tunnel

5.1.3 Velocity Board. A velocity board is a board painted with bands of contrasting colors to serve as a visual reference so that moving objects can be tracked against it, measured, and their velocity calculated. The velocity board for these tests was placed behind the loaded borehole to serve as a scale for the camera software to reference. The velocity board, pictured in Figure 5.2, was a 4' x 8' sheet of 5/8" plyboard painted with 6" parallel alternating black and white stripes. The purpose of these stripes was to give the camera software a standard unit to use for calibration. It was necessary to have the screen visible in the initial frames of the high-speed recording to provide a frame of reference for the moving flyrock fragments. The only place this board was not used was during the three Belanger mat tests in Section 6.5. For these shots, vertical rock face behind the shots was painted to provide the scale needed because placing a velocity board was impractical at that blast location.

Figure 5.2 Velocity Board

The board was placed approximately 3' behind the blasthole during each flyrock test. Once it was in place, the board was set perpendicular to the camera and as plumb as

possible. This was done for the same reason as keeping the camera at a similar elevation. With the velocity board standing vertical, distortion of the scale reference is reduced. An average margin of error of +/- 4% in flyrock speeds was estimated, with the exception of tests 2, 2r, and 3, which had the camera placed within 50ft of the board and at a higher elevation. This placement of the camera was due to the rock-wall boundaries of the MST quarry blocking line-of-site of the blast if the camera was placed elsewhere. Once camera setup was complete and the velocity board in place, the borehole was loaded, the area cleared, and the test fired.

5.1.4 Loading and Initiation. The boreholes were loaded with $1\frac{1}{4}$" x 8" cartridges of Unimax TT dynamite. The bottom cartridge was primed using an EZ Det 25/350ms non-electric blasting cap by simply inserting the cap into the cartridge. The cartridges following the primed cartridge were loaded up to the desired height in the borehole so that they were seated atop each other in a continuous column. The cartridges were also tamped if the test required it, with the exception of the primed cartridge as per MSHA and OSHA regulations. Once the desired amount of explosives had been loaded, the hole was stemmed by hand with 3/8" pea gravel to the top of the borehole. Stemming the shot by hand allowed large pieces of rock in the stemming material to be discarded before they could not become caught in the hole and prevent a full column of stemming from being loaded. An electric starter cap was attached to the EZ Det to initiate the shot. Once the blasting lines were hooked up, the blast site was cleared and the shot initiated. On these initial tests, the camera was triggered via laptop manually. Since the total recording time was about 4 seconds, all 4 seconds were recorded post trigger. This method was adequate for capturing images of the flyrock's initial velocity. Once the tests were completed, the data was easily downloaded. More detailed information about the test configurations can be found in Appendix B, Table B1.

5.2 FLYROCK TEST RESULTS

Once the tests were completed, the results were evaluated. The measurements taken were initial maximum flyrock velocities and crater volume. The initial flyrock velocities were measured using the Phantom camera's image viewer program. This program plays the recorded videos and allows for velocity measurements from frame to

frame. The videos were scaled using the program to reference a background object of known size, in this case the velocity board. Once a scale had been established, the moving objects were referenced and the program calculated the difference in distance and time between frames to produce the measured flyrock velocities. Both the calibration and measurement of flyrock velocities were done in the section of video before blast vibrations moved the camera. Only the velocity of the leading fragments in each test was measured. This was to ensure that the velocities were a maximum value because these tests were not designed to account for average velocity of all projected fragments. The results for the observed flyrock velocities are listed in Table 5.1. This table lists the velocities of the projected rock fragments and, if visible, exhaust gasses exiting the borehole. These are listed next to the test number, powder column height and explosives amount.

Along with measuring projection velocity, crater volume was calculated. The diameter of the crater was measured to the nearest $\frac{1}{2}$ ft. using a stiff loading pole lain across the crater. The depth of the crater was measured by dropping a measuring tape from the loading pole to the bottom of the crater (top of the remaining borehole), to the nearest inch. These dimensions were used to calculate the volume of the blasted crater, assuming a conical crater shape with a volume of $\frac{1}{3}\pi r^2 h$, because the craters produced during these tests were mostly conical. These calculated values are shown in Table 5.2 against their estimated theoretical values. In the later tests, the gap between the calculated and theoretical values became larger. More detailed recorded data can be found in Appendix C, Table C1.

5.2.1 Observed Flyrock Velocities. 2000 frames per second was more than enough for capturing the flyrock, which had observed velocities ranging from 21 to 527fps. Test 2 had to be repeated because it didn't get caught on camera the first time due to operator error. The highest velocity of flyrock recorded was only 527ft/sec on one of the later tests that had a higher powder factor. This velocity was close to the adjusted theoretical initial projection velocity of around 560ft/sec determined in Section 3, Table 3.2. The first tests had lower velocities as a result of less explosives. This is an actual value and contradicts the estimates found using equation 5 because of the problems discussed in Section 3.5.2. The flyrock velocities increased over the test range with the

increase in the amount of dynamite used, as seen in Table 5.1. The first 4 tests, including the repeat test were shot to determine whether the next increment of explosives used in the testing would be safe to shoot. Tests 5,7,9 and 6,8, and 10 used the two highest amounts of dynamite used in the testing. Strangely enough, tests 5,7, and 9 averaged 10% higher flyrock velocities than those in tests 6,8, and 10 which used an additional 27% of dynamite at the same powder column height. The untamped powder column tests, 5, 7, and 9 averaged around 466ft/sec, while the tamped powder column tests, 6, 8, 10 averaged around 420ft/sec. At these speeds, the frame rate of 2000fps captured at least 4 frames for the velocities to be measured. This was beneficial if exhaust gasses and dust obscured some of the rocks during intermittent frames, or the rock was framed with a background of similar shade. The launch velocities measured were for the leading edge of the flyrock. Only the fastest fragment speed was measured. Since there was no practical way of accounting for the velocity of all projected particles, it was assumed that the launch velocity of the average fragment was half the highest observed velocity. These estimates were paired with the measured crater volumes to obtain a rough estimate for the amount of energy the blasting mats would be required to resist.

Table 5.1 Flyrock Initial Velocity

Test No.	Lbs.	Exp. Height ft	Gas V fps	Rock Vo fps	Gas/Rock V
1	2.25	3	437	120	3.65
2	2.75	3	x	x	x
2r	2.75	3	677	60	11.31
3	3	4	x	21	x
4	3.75	4	649	205	3.17
5	3.75	5	909	424	2.14
6	4.75	5	1353	386	3.51
7	3.75	5	1524	448	3.40
8	4.75	5	1677	500	3.36
9	3.75	5	1346	527	2.55
10	4.75	5	1463	373	3.92

Table 5.2 Crater Volume Estimations

Test No.	D ft	R ft	H ft	V ft^3	Theoretical V ft^3
1	2.00	1.00	0.50	0.52	0.675
2	4.00	2.00	0.75	3.14	1.375
2r	4.00	2.00	1.25	5.24	1.375
3	4.00	2.00	0.33	1.38	2.1
4	6.50	3.25	1.25	13.83	3.375
5	5.50	2.75	1.00	7.92	26.25
6	6.00	3.00	1.25	11.78	66.5
7	5.50	2.75	1.20	9.50	26.25
8	6.00	3.00	1.33	12.53	66.5
9	4.50	2.25	1.50	7.95	26.25
10	5.75	2.88	1.50	12.98	66.5

5.2.2. Measured Crater Volume and Estimated Energy. The craters formed by the test shots were measured to obtain the total volume of rock that a blasting mat would need to stop during a blast. Formed craters were measured by laying a loading pole across to measure its diameter, and then dropping a tape measure from the bottom of the loading pole to the top of the visible remaining borehole, as described at the end of Section 5.2. These measurements were then used to calculate the volume of a cone to approximate the volume of the crater. The crater volumes, shown in Table 5.2 and plotted in Figure 5.3, increase across the test range, with the exception of test 4 being the largest value.

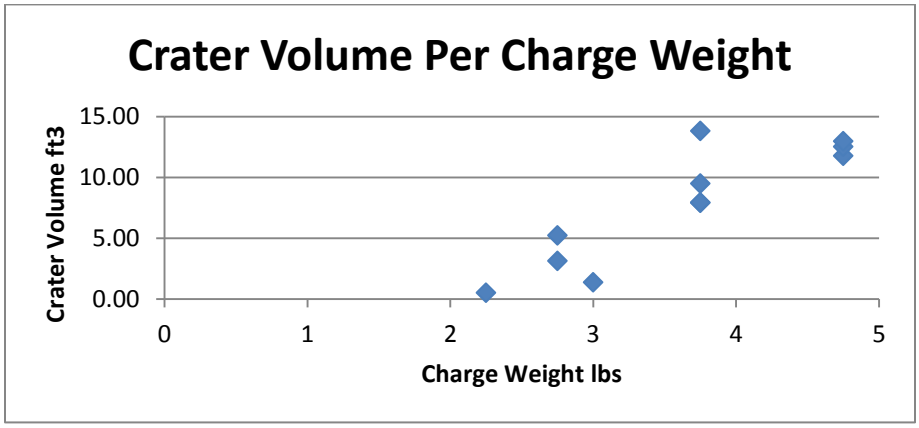

Figure 5.3 Crater Volume Plotted by Charge Weight

This was likely due to the large amount of dirt and clay near the top of the borehole instead of rock. Even though the largest measured crater volume occured at the second highest charge weight, 3.75, the highest average crater volume belonged to the group of tests with the highest charge weight, 4.75lb. Test 3 had the second lowest crater volume, which could be attributed to the borehole's close proximity to previously blasted rock. This would allow the blast energy to disperse more quickly throughout the rock by way of existing fractures. Tests 5,7, and 9 averaged 8.5ft^3 of crater volume, and tests 6,8, and 10 averaged around 12.4ft^3, nearly 1.5 times that of tests 5,7, and 9. Tests 6,8, and 10 were still only about 1/5 the value of those predicted in Section 4, Table 3.1. For these tests averaging 12.4ft^3, this is a scaled crater volume of 2.61ft^3/lb. This SCV is about 7 times of that used in Table 3.1 but represents roughly a 40% increase in the SDOB. The crater volumes were multiplied by a density of 160lb/ft^3 for limestone to provide the weight of the rock that would have occupied the crater. This weight was paired with the measured velocities and halved to give a representative energy that a blasting mat would encounter. The velocities were halved for these calculations in a similar manner to Section 4. These energy estimations are shown in Table 5.3.

Table 5.3 Estimated Blast Energy

Test No.	Energy ft lbs
1	5,019
2	x
2r	25,071
3	2,371
4	226,408
5	268,597
6	363,758
7	340,714
8	500,949
9	335,200
10	387,794

Tests 6, 8, and 10 averaged the highest energy, around 417,500 ft lb/sec. This is 33% higher than the average of tests 5, 7, and 9. Even though the average velocities for

Tests 5, 7 and 9 were higher, the differences in blasted volume between these tests set apart the two test setups. This made it easy to determine the test setup that would rigorously test the blasting mats. Figure 5.4 is a plot of calculated energy per charge weight. In Figure 5.3, the crater volume for one of the 3.75lb shots was the largest value. Figure 5.4 shows that the larger crater volume did not necessarily account for more energy in the tested rock mass. In this plot, the largest charge size, 4.75lb, is shown to have a much larger calculated energy. This charge size was selected for testing the blasting mats.

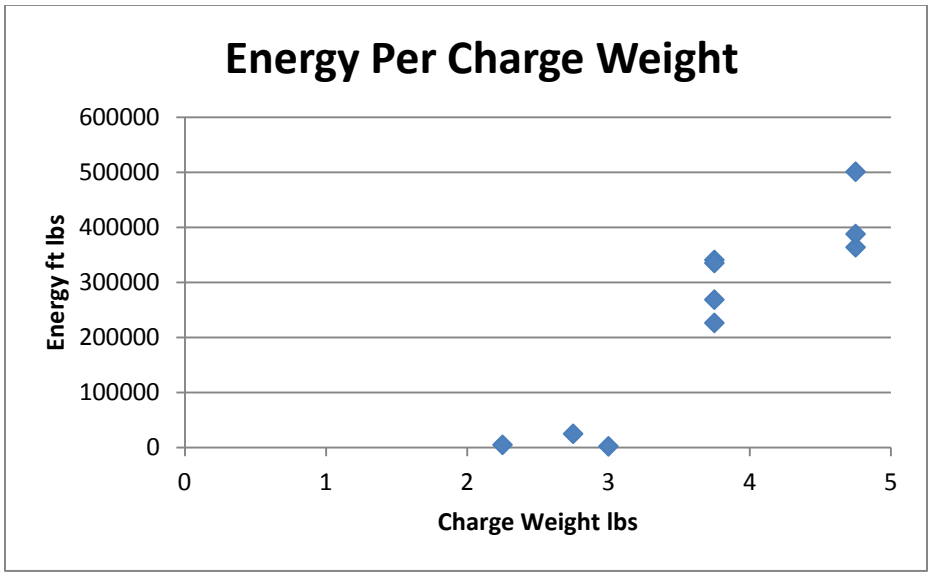

Figure 5.4 Calculated Energy per Charge Weight

5.3 SUMMARY OF FLYROCK TESTING

Upon test completion, the flyrock test data was found to be representative of the velocity and volume estimates that were predicted in Section 3. The crater volumes that were determined directly from SDOB equations in Table 3.1 were very close to the actual value. That portion of the model is very sensitive to changes in the SDOB and even a change as small as 5% in SDOB could mean double or half the scaled crater volume. A

small change in SDOB of a test could have a large influence on the volume of rock produced during blasting. The measured flyrock velocities however were representative of the determined velocity in Table 3.2, which was based on the optimal SDOB of 1.6 and had a scaled crater volume over seven times that of the actual tests. This means that the speed of the projected fragments was representative of a situation where a much larger crater was formed, even though a small crater was actually produced. More work will be needed to determine why this occurs and also how the performance of these tests changes in different rock masses. At this point, the actual values that the mats would encounter in the tested rock mass had been measured and they could be tested. The test setup averaging the largest energy was the 5' powder column with 4.75lb of tamped dynamite. This setup was representative of either an initial trenching hole, or one following a misfire where there was rock confinement in all directions and the blast energy would be directed upwards. This was selected to test the tractor-tread blasting mats and their performance. A Belanger style blasting mat was tested the same way for comparison and the performance of both mats was assessed and compared accordingly. The next section covers the blasting mat tests.

6. BLASTING MAT TESTS

6.1 INTRODUCTION

In the previous section, the blast design for testing the blasting mats was established. This section describes the testing and comparison of the two mats, the author's tractor tread mat, and the Belanger style. The tractor tread mat was tested as well as a Bellanger style mat for a control. The results of these tests are discussed along with the mats' performances, and the suitability of a blasting mat made from rubber tractor tread determined.

6.2 TEST SETUP

In Section 5, flyrock conditions were measured and the blast configuration with the most energy imparted to thrown rock fragments was selected. This configuration was used to test the blasting mats in which single holes were loaded and tamped so that each contained 4.75lbs of dynamite at a powder column height of 5.' The only differences in procedure between the previous flyrock tests and the blasting mat tests were the application of the blasting mats and the use of a remote camera trigger.

The blasting mats were laid on top of the shot in the configuration shown in Figure 6.1. They were placed as centered over the borehole to ensure that the most energy was imparted to the mat and it was done in a symmetrical manner. The tractor-tread mat was laid with the tread side against the ground. Care was also taken so that the blasting mats were not dragged across the non-electric tubing to avoid damage and the risk of a cut-off. The fasteners used to pin the tractor-tread mats together leave an extended portion at either end of the cable bolts which can snag or cut blasting lines if dragged across a shot. Once the mats were placed, the remote trigger was hooked up and the shots initiated in the same manner as the previous tests.

Figure 6.1 Blasting Mat Centered Over Borehole

For the flyrock tests, the Phantom camera was triggered using the laptop. One test had to be repeated because of operator error using this method. To ensure that all the blasting mat tests were captured, a remote trigger was used to set off the camera. This trigger used a break circuit consisting of a single loop of wire connected to a signal box that provided the trigger signal to the camera. This single loop of wire was placed in the surface connector for the non-electric cap. When the surface connector fired, it broke the circuit and triggered the camera via the signal box. As a 25/350 EZ Det was used with a 350ms downhole delay, a 350ms pretrigger was used to ensure the event was captured. The remote trigger allowed for more consistent recordings of the blasting mat tests. Performance of the blasting mats was judged on launch velocity, and durability of the mat. The mats also had to perform their jobs of mitigating the flyrock hazard and allowing transmission of exhaust gasses.

The original test series consisted of six tests of the tractor tread mat and three for the Belanger mat. The tractor tread mat tests were doubled to determine its durability. The Belanger style mat, borrowed from Twehouse Construction, is a regularly used

design of blasting mat in the blasting industry and did not need to be subjected to additional tests. Three tests were also planned for the tractor tread mat with the Belanger mat on top of it. The Belanger mat did not survive testing on its own. Extra strips of tractor tread were used to provide extra weight for the tractor tread mat instead. These tests still had a weight comparable to the Belanger mat. More detailed information about the test setup is found in Appendix B, Table B2.

6.3 BLASTING MAT TEST RESULTS AND ANALYSIS

The initial velocities of the blasting mats were recorded and measured the same way that the flyrock test velocities were recorded and measured. The velocities obtained from these tests are shown in Table 6.1. The tests referred to in this table as Tread + Weight are the tractor tread mats with additional weight on top, as described in the previous paragraph. More detailed data can be found in Appendix C, Table C2.

Table 6.1 Observed Blasting Mat Velocities

Test No.	Mat type	Mat Vo fps
1	Tractor Tread	63.41
2	Tractor Tread	17.44
3	Tractor Tread	24.46
4	Tractor Tread	36.66
5	Tractor Tread	26.14
6	Tractor Tread	68.60
7	Belanger	53.04
8	Belanger	50.40
9	Belanger	53.16
10	Tread + Weight	26.01
11	Tread + Weight	50.89
12	Tread + Weight	27.47

6.4 TRACTOR TREAD MAT TESTS

The first six tests, using just the tractor tread mat, yielded a variety of velocities. Each of these tests managed to prevent the rock fragments from leaving the blasting site. However, the tractor tread mats were thrown high into the air and out of the view of the camera on the first three tests. In the Phantom camera video recordings, explosion gasses can be seen trying to escape through the gaps between the treads as illustrated in Figures 6.2 and 6.3. These stills, taken from test 3, were 5ms apart.

Figure 6.2 Gasses Beginning to Exit Blasting Mat During Test 3

Figure 6.3 Gasses Exiting Blasting Mat after 5ms of Expansion During Test 3

Although the mat performed adequately, on the 4th test of the tractor tread mat the center cable connecting the bottom and middle strips of tread pulled through the middle strip. The rock was still contained to the blast area. A closer look at the high speed video of the 4th tractor tread test shows that the bolt pulled out because of this need to vent gasses. Enough force was produced that the 3" washer and ferrule was pulled through the 1" hole in the tread. The bolt was examined after the test and was found to be completely intact. It was left out of the mat for the next two tests to allow for better venting. Tests 5 and 6 had the bolts to the left and right of the pulled bolt also came apart. In each those tests, a ferrule slipped off the end of one of the cables. With these bolts removed, the aperture between the two strips of tread could open up and vent gasses very quickly. The only downside is that with three bolts missing, only the two end bolts held the middle and lower strip together. The size of that aperture could potentially allow flyrock to pass through it. The mat was not repaired in between these tests to see how much abuse it could take. With some of its integrity gone, the tractor tread mat didn’t

completely disintegrate, or lose large portions of its surface area. It still covered the same amount of ground.

None of the bolt holes punctured in the treads were ripped out during these tests. The bolts could be reinstalled using the same holes whenever a repair was needed. This shows that the mat does not lose its usefulness for lack of a couple bolts, although larger washers were needed for the bolts that pulled through or apart. As long as it still has a couple of bolts holding it together, it will still work or can be easily repaired.

6.5 BELANGER MAT TESTS

After the six tractor tread tests, the performance of Belanger style mat that had been borrowed from Twehouse Construction was evaluated for comparison. Three tests were conducted using this mat. This mat adequately stopped almost all of the flyrock from leaving the site, but a steel cable that was binding the mat snapped on each test. Three cables in a row snapped, starting with an outside cable and worked toward the center. With each successive test, large amounts of the rubber tire strips that comprised the bulk of the mat could be seen flying out of the view of the camera. Rocks can also be seen flying through the gaps made from this loss of bulk material. The cable was examined and found to be unusually brittle and weathered. It is possible this material was recycled from scrap cables. In an attempt to stop further disintegration, cable clamps were placed on the ends of the broken cables so that no more pieces could unthread from the broken cable. This repair did not work. Not only did another cable break during the next test, but the cable clamps on the ends of the existing broken cables were broken off themselves. After the three tests, about 525lb of rubber had been lost from the mat, leaving only 77% of its original weight. At this point the mat was determined to be beyond repair and of no further use. It had lost a large portion of its bulk and was only bound by half of the steel cables it had to begin with. This was one of the problems discussed with the Belanger style mat in Section 2.1.1. It becomes even more a problem when these mats are often constructed of recycled scrap cables.

6.6 TRACTOR TREAD MAT PLUS WEIGHT TESTS

Before these tests, the original tractor tread mat was refurbished. Three of the 1' cable bolts were no longer binding the mat and needed to be reset. The cable bolts were reinstalled with the addition of a 6" rock bolt plate on both ends between the treads and the 3" washers. This 6" plate added five times the surface area of the previous bolt and ensured that bolts would not pull through as in Test 1. The center bolt was left out to allow the mat to vent, but the two on either side were replaced. The repairs only took 45 minutes after finding the tools for the job. In comparison trying to re-string the Bellanger mat would take many hours to complete. In addition, once the new cable bolts were installed, the sharp pieces of cable sticking up out of the ferrules were ground off to keep sharp edges from severing blasting lines, and for handling safety.

The tractor tread mat was applied the same way as it was in tests 1-6, but three more tread strips were added on top to provide weight comparable to the Belanger style mat. The three strips doubled the 1260lb of the tractor tread mat to 2520lbs, which was close to the Belanger mat's starting weight of 2360lbs. There were three tests done on this mat setup. Of the three tests conducted, none of them left the frame of the camera. They were the most uneventful mat tests conducted in this project. With all the tests completed, the mat designs were compared and the effectiveness of the tractor tread assessed.

6.7 SUMMARY OF MAT TESTS

The conditions the blasting mats were subjected to were very severe. Both mats incurred damage of some degree during the testing, often related to their method of binding. The tractor tread mat performed well in the battery of tests it was subjected to. Even with the loss of binding, the mat was still able to stop the flyrock. It withstood the testing better than the Belanger mat, although some minor modifications had to be made to increase the durability and longevity of the mat.

The addition of extra weight helped the performance of the mat greatly. By doubling the weight, the mats were not launched into the air. To adequately protect from flyrock, the weight of tractor tread mats needed to adequately protect from flyrock should be approximately the same as the rubber tire mats. This means twice as much tractor tread material, but if it becomes damaged, that material is easily gathered and repaired.

After all the tests were completed, there was not a tear or chunk missing from the tractor treads. The only part of the mat that needed repair and modification was the method of binding. The ferrule and wedge fastener worked well in holding on the ends of the cables but a larger bearing surface area was needed to prevent them from pulling through the treads. A change that was not made but could add integrity to the mat fasteners would be to use an epoxy or resin to permanently set the ferrules on the ends of the cables. This would eliminate the problem of slippage in the ferrules as shown in Tests 5 and 6. Aside from that, these mats were sufficiently durable and withstood the test conditions. In the case of repairs, they were both quickly and easily repaired in the field.

This thesis has proven that used rubber tractor treads are a recycled material that can reliably be used to construct a blasting mat. They are durable enough to withstand the rigors of the blast conditions, and with proper application, can provide adequate protection from flyrock.

7. CONCLUSION OF THESIS

The test development for assessing blasting mat performance was intensive. The following conclusions were obtained for the blasting mat test setup:

- There was no current method found for testing blasting mats.
- A test was developed using the components of crater formation, fragmentation, and initial velocity to estimate the blasting forces a mat would encounter.
- The test was representative of real world conditions. Loading of blastholes was similar to what would be found on an actual trenching job.
- The test was very rigorous. Both blasting mats tested incurred damage, and the Belanger mat was destroyed beyond repair.

Once the test had been designed the blasting mats were put to the test. From this testing, the following conclusions were obtained for the tractor tread material:

- The tractor tread mat withstood the blast conditions better than the Belanger style mat which was destroyed. The tractor tread material did not incur damage during blasting. It still needs to be used in an industrial setting to determine its longevity.
- The tractor tread mat was too lightweight to use by itself. It needed additional weight, probably another mat of the same construction.
- The fasteners of the tractor tread mat work well, even with recycled cable, as long as there are large enough washer plates to prevent them from slipping through the treads.
- Epoxy or some sort of resin should be used to keep the ferrules on the end of the cable bolts.
- In the event that a repair is needed, little time and effort is involved in fixing the tractor tread mat.

With the completion of this thesis, the rubber tractor tread blasting mats can be deemed satisfactory for blasting applications. There is now also a standardized test that can be used to determine the feasibility of other recycled materials for use as blasting mats.

8. FUTURE WORK

The following recommendations are made based on the results found in this study:

- An analysis needs to be done to compare the costs of constructing and using the tractor tread mats in an industrial environment including mechanical cutting and machining versus explosives cutting methods.
- More work needs to be done to build a more accurate model of flyrock conditions. The flyrock velocities as well as mean particle size need to be reexamined to establish their correlation to blasting conditions found at SDOB greater than 1.6.
- The flyrock model and actual testing conditions need to be evaluated in geologic conditions other than those used in this project. Different rock types would produce different crater shapes and sizes as well as different flyrock conditions.

APPENDIX A.
SAMPLE CALCULATIONS

This appendix goes through the sample calculations used Section 3 for in estimating flyrock conditions before blasting. These calculations will assume:

6' deep blasthole, 1.5" in diameter
5' tamped powder column height, then 1' of stemming material
Rock density of 2560kg/m^3, or 160lb/ft^3
Loaded with 1 1/4" x 8" sticks of dynamite at 1.55g/cc, with 94% TNT equivalency
The total explosives weight is 4.75lb

The scaled depth of burial of the shot is the first calculation made. It is done using equation 3 and 4 in Section 3.

$$SDOB_{U.S.} = \frac{Is + 0.042 * m * d}{0.305 * (m * d^3 * \rho e)^{0.333}}$$

Where:
$SDOB_{U.S.}$ = U.S. Scaled depth of burial (feet/pound^3)
I_s = Stemming length (feet)
d = Blasthole diameter (inches)
m = Contributing charge length factor
ρ_e = Explosive density (grams/centimeter^3) (ISEE, 2011)

The contributing charge length factor is

$$m_{U.S.} = \frac{12 * Ic}{d}$$

Where:
$m_{U.S.}$ = Contributing (US) charge length factor (blasthole diameters)
I_c = Charge length (feet)
d = Blasthole diameter (inches) (ISEE, 2011)

By filling in equations 3 and 4, the scaled depth is

$SDOB_{U.S.} = \frac{1+0.042*40*1.5}{0.305*(40*2.25*1.55)^{0.333}} = 2.23 yd/lb^3$

From here, Roth's chart (Figure 3.1) is used to indicate the scaled crater volume. This project assumed that the rock would behave like the sandstone in Roth's study. Using the sandstone reference line, Roth's chart gives a scaled crater volume of $5yd^3/lb$. This is multiplied by the charge weight, 4.75lb, to obtain $23.75yd^3$ as the crater volume.

From here a few U.S. to metric conversions need to be done. The charge weight of 4.75lbs needs to be changed to a TNT equivalent charge in kg. This is done by multiplying the weight by 0.45 to convert to kg and then 0.94 to make it a TNT equivalent weight. The result for this calculation is about 2.

Crater volume also needs to be multiplied by 0.03 to convert it to m^3. The resulting crater volume is $0.67m^3$.

Next, mean fragment size is calculated using equation 1.

$$< x > = A(\frac{Vo}{Q})^{4/5} * Q^{(\frac{1}{6})}$$

Where:
< x > = mean fragment size (cm)
A = correction factor; assume 7 for medium hard rocks
Vo = volume of blasted rock (m^3)
Q = TNT equivalent of the explosives weight (kg)

Equation 1 filled in

$< x > = 7(\frac{0.67}{2})^{4/5} * 2^{(\frac{1}{6})} = 3.28$ cm

With the mean fragment size determined, flyrock velocity is determined next using equation 5.

$Vo = 10 (d/ x_f) * (2600/ \rho_r)$

Where:

Vo = initial projection velocity (meters/second)

d = diameter of borehole (inches)

x_f = fragment size (meters)

ρ_r = rock density (kilograms/meter^3)

Equation 5 filled in

$Vo = 10 (1.5/ 0.0327) * (2600/ 2560) = 466$m/s

Where:

Vo = initial projection velocity (meters/second)

d = diameter of borehole (inches)

x_f = fragment size (meters)

ρ_r = rock density (kilograms/meter^3)

Finally, the velocity and fragment size are used to calculate the estimated trajectory of the fragment using equations 6,7, and 8.

$Z = (1/b_d)*\ln(1+b_d V_o t)$

$Y=(1/b_d)*\ln ((e \wedge (2*t*\sqrt{(b_d*g)})+1) / (2 * e \wedge (t * \sqrt{(b_d * g)}))$

$b_d=1.3/(x_f*\rho_r)$

Where:

V_o = Projection Velocity (meters/second)

t = Time after launch of the fragment (seconds)

g = Acceleration due to gravity (9.81 meters/second^2)

x_f = Fragment Size (meters)

ρ_r = Rock density (kilograms/meter^3)

Z = Distance measured along the line of the initial projection angle (meters)

Y = Vertical distance measured from the line of initial projection (meters) (ISEE, 2011)

These equations are filled out and solved with respect to time where Z is the hypotenuse of a 45 degree right triangle. This uses the constraint where X=Y at time T.

$Z = (1/b_d)*\ln(1+b_d * 466 *t)$

$Y=(1/b_d)*\ln ((\ e \wedge (\ 2*t*\sqrt{(\ b_d*9.8))+1) / (\ 2 * e \wedge (\ t * \sqrt{(\ b_d * 9.8\ )}\ )$

$b_d=1.3/(.0327*2560) = 0.016$

Where:

V_o = Projection Velocity (meters/second)

t = Time after launch of the fragment (seconds)

g = Acceleration due to gravity (9.81 meters/second^2)

x_f = Fragment Size (meters)

ρ_r = Rock density (kilograms/meter^3)

Z = Distance measured along the line of the initial projection angle (meters)

Y = Vertical distance measured from the line of initial projection (meters) (ISEE, 2011)

The resulting flyrock range from solving these equations in Microsoft Excel is

Z=266 m

Y=188 m

X = 188m

T=9.35s

With this calculation, the flyrock estimations are complete for this test setup.

APPENDIX B.
TEST CONFIGURATIONS

This appendix contains the test conditions that were used in both the flyrock tests and the mat tests.

Table B1 Flyrock Test Configurations

Test No.	Lbs.	Exp. Height ft	Distance to Camera ft	Temperature F
1	2.25	3	82	34
2	2.75	3	39	34
2r	2.75	3	48	34
3	3	4	41	34
4	3.75	4	107	34
5	3.75	5	106	34
6	4.75	5	107	73
7	3.75	5	110	73
8	4.75	5	102	73
9	3.75	5	112	73
10	4.75	5	110	73

Table B2 Blasting Mat Test Configurations

Test No.	Lbs.	Exp. Height ft	Distance to Camera ft	Temperature F	Mat Used	Additional Weight
1	4.75	5	112	65	Tractor Tread	
2	4.75	5	105	65	Tractor Tread	
3	4.75	5	111	65	Tractor Tread	
4	4.75	5	117	45	Tractor Tread	
5	4.75	5	126	45	Tractor Tread	
6	4.75	5	129	45	Tractor Tread	
7	4.75	5	65	52	Belanger	
8	4.75	5	65	52	Belanger	
9	4.75	5	72	52	Belanger	
10	4.75	5	76	70	Tractor Tread	x
11	4.75	5	80	70	Tractor Tread	x
12	4.75	5	78	70	Tractor Tread	x

APPENDIX C.
RAW RESULTS

This appendix contains the raw data for the flyrock and blasting mat tests. The velocity calculations were done in the Phantom camera's video software. The video frame numbers where the measurements were taken is included.

Table C1 Flyrock Test Results

Test No.	Gas Frame 1	Gas Frame 2	Gas Distance ft	Rock Frame 1	Rock Frame 2	Rock Distance ft
1	1453	1465	2.1823	1468	1493	1.4942
2	N/A	N/A	N/A	N/A	N/A	N/A
2r	989	997	2.7012	1001	1124	3.6725
3	No Gas	x	x	2702	3038	3.5936
4	2495	2503	2.5914	2509	2540	3.1655
5	1727	1732	2.2669	1727	1748	4.4414
6	1641	1644	2.0256	1644	1670	5.0061
7	1267	1270	2.2814	1270	1308	8.4956
8	1057	1061	3.3459	1075	1089	3.4889
9	4822	4827	3.3579	4842	4858	3.6799
10	1283	1287	2.9189	1306	1322	2.98

Table C1 Flyrock Test Results Continued

Test No.	Gas V fps	Rock Vo fps	Ratio	Crater Diameter	Crater Depth
1	437.4573	119.8091	3.651286	2.00	0.50
2				4.00	0.75
2r	676.8444	59.85193	11.30865	4.00	1.25
3		21.43922		4.00	0.33
4	649.3221	204.6903	3.172217	6.50	1.25
5	908.8403	423.9518	2.143735	5.50	1.00
6	1353.452	385.9594	3.50672	6.00	1.25
7	1524.42	448.1517	3.401572	5.50	1.20
8	1676.765	499.5522	3.356537	6.00	1.33
9	1346.214	526.9003	2.554969	4.50	1.50
10	1462.747	373.3497	3.917899	5.75	1.50

Table C2 Blasting Mat Results

Test No.	Mat Frame 1	Mat Frame 2	Mat Distance ft	Notes	Mat V fps
1	1356	1484	4.0489		63.407568
2	1132	1351	1.9054		17.44008
3	1172	1683	6.2342		24.455361
4	1161	1442	5.1396	Center Pin Pull Out	36.664152
5	1116	1626	6.6508	2nd Pin Pull out	26.140716
6	1070	1194	4.2436	3rd Pin Pull out	68.600049
7	697	854	4.154	Cable 1 Broke	53.038923
8	707	1011	7.6434	Cable 2 Broke	50.399538
9	684	924	6.3643	Cable 3 Broke	53.156082
10	690	981	3.7759		26.009886
11	690	783	2.361		50.890077
12	690	861	2.3433		27.469449

BIBLIOGRAPHY

Arcand, L. H. (1982). *Patent No. 4315463.* United States.

Belanger. (1967). *Patent No. 3331322.* United States.

Berg, E. H. (1970). *Patent No. 3539135.* United States.

Cason, V. (2012, July 6). (M. Coy, Interviewer)

Cooper, P. W. (1996). *Explosives Engineering.* New York, New York: Wiley - VCH.

Crook, C. A. (1996). *Patent No. 5482754.* United States.

Cunn, A. (1970). *Patent No. 3648613.* United States.

Dyno Nobel (2003).*Explosives Engineers' Guide.*Salt Lake City,Utah:Dyno Nobel Inc.

Goldberg, J. (1989). *Patent No. 4801217.* United States.

ISEE. (2011). Flyrock. In J. F. Stiehr, *ISEE Blaster's Handbook 18th Ed.* (pp. 383-410). Cleveland, Ohio: International Society of Explosives Engineers.

Kuznetzov, V. (1973). The Mean Diameter of the Fragments Formed by Blasting Rock. *Journal of Mining Science, Volume 9, Issue 2* , 144-148.

Lewis, D. L. (1974). *Patent No. 3793953.* United States.

Mascus. (n.d.). Retrieved 2014, from Mascus.com: http://www.mascus.com/agriculture/used-tracked-tractors/john-deere-camoplast-tracks-to-fit-john-deere-8000t-9000t/fuegdlft.html

Mazella, J. A. (1975). *Patent No. 3870256.* United States.

Meagher, W. K. (1976). *Patent No. 3945319.* United States.

Robertson, T. A. (1976). *Patent No. 3943853.* United States.

Roth, J. (1979). *A Model for the Determination of Flyrock Range as a Function of Shot Conditions.* Los Altos, California: Management Science Associates.

Thomas, B. (2014, April 10). Sydenstricker Sales. (M. Coy, Interviewer)

Wikner, P. F. (1968). *Patent No. 3371604.* United States.

VITA

Matthew Kurtis Coy was born in 1987. He grew up in rural Northeast Missouri, and spent a lot of his time outdoors. During his school years, he participated in academic and athletic extracurricular activities. He was also an active member of the local 4-H youth organization, participating in shooting sports and many other activities. Matthew graduated from Highland High School in May 2006. From there he went on to the University of Missouri, Rolla (now Missouri S&T) to pursue an education in explosives. At college, Matthew became involved in many organizations, primarily MS&T's Mucking and Pyrotechnics programs. Both of these programs involved lots of hard work and dedication but have provided him with many opportunities to travel and see places many people do not have the opportunity to.

Matthew graduated from MS&T with a Bachelor of Science in Mining Engineering in December 2010. Since then, he has been working to finish his graduate degrees in Explosives Engineering. At the time of finishing this thesis, he is an instructor for the Proximate and Display Pyrotechnics classes, a graduate teaching assistant for the Advanced Blasting class, and is still an active member of the Mucking team.